UCRL-11568
c.2

University of California

Ernest O. Lawrence Radiation Laboratory

TWO-WEEK LOAN COPY

This is a Library Circulating Copy which may be borrowed for two weeks. For a personal retention copy, call Tech. Info. Division, Ext. 5545

SIGMA-PION FINAL STATE INTERACTIONS

Berkeley, California

UCRL-11568
c.2

DISCLAIMER

This document was prepared as an account of work sponsored by the United States Government. While this document is believed to contain correct information, neither the United States Government nor any agency thereof, nor the Regents of the University of California, nor any of their employees, makes any warranty, express or implied, or assumes any legal responsibility for the accuracy, completeness, or usefulness of any information, apparatus, product, or process disclosed, or represents that its use would not infringe privately owned rights. Reference herein to any specific commercial product, process, or service by its trade name, trademark, manufacturer, or otherwise, does not necessarily constitute or imply its endorsement, recommendation, or favoring by the United States Government or any agency thereof, or the Regents of the University of California. The views and opinions of authors expressed herein do not necessarily state or reflect those of the United States Government or any agency thereof or the Regents of the University of California.

Research and Development

UCRL-11568

UNIVERSITY OF CALIFORNIA
Lawrence Radiation Laboratory
Berkeley, California

AEC Contract No. W-7405-eng-48

SIGMA-PION FINAL STATE INTERACTIONS

Yu-Li Pan

(Thesis)

August 1964

Reproduced by the
Technical Information Division
directly from author's copy

CONTENTS

Abstract		iii
I.	Introduction	1
II.	Literature Survey	3
III.	Theory	7
IV.	Experimental Procedures	11
V.	Data Processing	14
VI.	Preliminary Checks	18
VII.	Production Cross Sections	25
VIII.	Phase Space and Resolution	28
IX.	Results and Discussion	32
	A. Fermi Momentum Distribution	32
	B. Y-2π System	32
	C. Lambda-two-pion Events	36
	D. $\Sigma^+ \pi^- \pi^-$ Events	40
	E. $\Sigma^- \pi^- \pi^+$ Events	46
X.	Conclusion	66
Acknowledgments		68
Footnotes and References		69

SIGMA-PION FINAL STATE INTERACTIONS

Yu-Li Pan

(thesis)

Lawrence Radiation Laboratory
University of California
Berkeley, California

August 1964

ABSTRACT

Sigma hyperons produced with two pions by 1.15 BeV/c K^- on neutrons in the 30-inch propane bubble chamber[1] were used to study final state interactions of the particles. The production of Y_1^* (1385) on protons in carbon was also studied.

We observed the Y_1^* (1385), Y_0^* (1405), and Y_0^* (1520). In addition, the data indicates the existence of a T = 2 sigma-pion resonance at a mass of 1415 ± 16 MeV, with full-width at half-maximum of 50 MeV or less. The spin and parity of this resonance have not been determined. Further, the data shows a possible resonance in the region of 1750 MeV in the reactions $\Lambda\,\pi^-\,\pi^+$ and $\Sigma^\pm\,\pi^\mp\,\pi^-$. This may be associated with the decay of the 1765 MeV Y_1^* into these channels.[2]

The production cross sections for $\Sigma^-\,\pi^-\,\pi^+$ and $\Sigma^+\,\pi^-\,\pi^-$ reactions are 0.51 ± 0.07 mb and 0.45 ± 0.07 mb, respectively.

I. INTRODUCTION

Since the discovery of the Y_1^* (1385),[3] and the subsequent spin determination,[4] there has been continuous theoretical speculation regarding the existence of a Y_2^*.

Dowell et al.[5] observed a peak at a mass of 1550 ± 20 MeV, which may have an isotopic spin of 2. But subsequent experiments have failed to confirm their finding.[7-12] These experiments will be discussed in detail in the next section.

In the present experiment, a search has been made for $\Sigma\pi$ resonances with T = 2 in the available energy region. The reaction studied is of the type

$$K^- + n(c) \rightarrow \Sigma^- + \pi^- + \pi^+ + \text{recoils} \qquad (1)$$

where n(c) means neutrons embedded in the carbon nucleus. This reaction is favorable for the observation of a T = 2 resonance for the following reasons:

1) A Y_2^* should decay into a Σ^- and a π^- at least part of the time. Both of these particles can be seen in the bubble chamber.

2) If T_3 is the Z component of the isotopic spin, then the ratio of the amplitudes of $T_3 = -2$ to $T_3 = 0$ for a Y_2^* decay is 6 to 1 as required by the Clebsch-Gordan coefficients.

3) If a Y_2^* exists, it is most easily produced from a T = 1 initial state. The K^-p system is a mixture of T = 0 and T = 1 states. But the K^-n system is a pure T = 1 state.

The reaction

$$K^- + n(c) \rightarrow \Sigma^+ + \pi^- + \pi^- + \text{recoils} \qquad (2)$$

does not give any information concerning a Y^* T = 2 resonance, but has

been studied for completeness.

Investigation was concentrated on categories(1) and(2) where the particles associated with K^-n events could be observed in sufficient abundance. K^-p interactions have been investigated thoroughly in previous experiments[9-11] and were not studied here.

Since the only known lambda-pion resonance in this region is the Y_1^* (1385), we studied the reaction

$$K^- + p(c) \rightarrow \Lambda + \pi^- + \pi^+ + \text{recoils} \qquad (3)$$

to see how a well known resonance is produced in carbon.

II. LITERATURE SURVEY

The existing experiments can be put into the following three classes: A. associate production, B. K^-p reactions, and C. K^-n reactions.

A. Associate Production

In a counter experiment, Dowell et al.[5] measured the cross section for K^+ production by negative pions on protons at 0 degree with a fixed K^+ momentum of 0.94 BeV/c. The pion momentum was varied from 1.3 to 2.4 BeV/c. Since the cross section for any two-particle scattering increases when new outgoing channels become energetically possible, the cross section for K^+ production should rise when Σ^- or Y_1^{*-} (1385) is produced with the K^+. Accordingly, they found peaks in the cross section when the missing mass reached 1197 MeV and 1385 MeV. The missing mass is calculable from the momenta of the incoming π^- and the observed outgoing K^+.

In addition to the two peaks noted above, they also observed a third enhancement at a mass of 1550 ± 20 MeV, which must have an isotopic spin of 1 or 2 since it is made with a K^+.

Since the experiment of Dowell et al., a $T = \frac{1}{2}$ resonance in the π^-p system at 2.1 BeV/c was found by Diddens et al.[6] The effect observed at 1550 MeV may be due to this pion-nucleon resonance.

Alexander et al.[7] and Kalbfleisch et al.[8] studied the reactions:

$$\pi^- + p \rightarrow \Sigma + \pi + K \qquad (4)$$

$$\pi^- + n \rightarrow \Sigma^- + \pi^- + K^+ \qquad (5)$$

The pion momentum was varied from 1.89 BeV/c to 2.36 BeV/c. In reaction (4), they observed Y_0^* (1405), Y_0^* (1520), and K^* (885). In reaction (5), they found that K^* (885) dominated the reaction. No resonance with isotopic spin of 1 or 2 was found in the region below 1900 MeV.

B. K^-p Reactions

These experiments can be classified into two types: 1) sigma-three-pion, and 2) sigma-two-pion.

1. Sigma-three-pion

The only two channels of this reaction that can be used to detect a T = 2 resonance are:

$$K^- + p \rightarrow \Sigma^+ + \pi^+ + \pi^- + \pi^- \quad (6)$$

$$K^- + p \rightarrow \Sigma^- + \pi^- + \pi^+ + \pi^+ \quad (7)$$

Alston et al.[9-11] studied these reactions extensively. The K^- momentum was varied from 1.15 BeV/c to 1.70 BeV/c. They found the Y_0^* (1405) at 1.15 BeV/c.[9] But the data at this momentum was limited by statistics. The data at 1.22 BeV/c,[10] 1.51 BeV/c,[10,11] and 1.70 BeV/c[11] was dominated by the production of Y_0^* (1405) and Y_0^* (1520). In addition, the data at 1.51 BeV/c and 1.70 BeV/c showed some Y_1^* (1660) production in the sigma-two-pion system. The fit to the phase space was bad at 1.70 BeV/c. Small enhancements above phase space were observed in the 1450 MeV region in the $\Sigma^+ \pi^+$ and $\Sigma^- \pi^+$ systems. These were not statistically significant. No T = 2 resonance was observed in any of these experiments.

2. Sigma-two-pion

The reactions which can be studied are:

$$K^- + p \rightarrow \Sigma^- + \pi^+ + \pi^\circ \quad (8)$$

$$K^- + p \rightarrow \Sigma^+ + \pi^- + \pi^\circ \quad (9)$$

$$K^- + p \rightarrow \Sigma^\circ + \pi^- + \pi^+ \quad (10)$$

In these reactions, one cannot observe the $T_3 = 2$ component of a T = 2 resonance. The production of a T = 2 Y^* in the above channels must come from a T = 1 initial state. The K^-p system is a mixture of T = 1 and

T = 0 states.

Bastien et al.[12] studied these reactions with K^- momenta of 760 MeV/c and 850 MeV/c. Although their data was low on statistics, they observed broad enhancements in the 1400 MeV region in the $T_3 = 0$ and $T_3 = |1|$ channels. The enhancement in the $T_3 = 0$ system was explained as Y_0^* (1405) production. But the larger and sharper enhancement in the $T_3 = |1|$ channel was explained as due to the decay of the Y_1^* (1385).

Alston et al.[9-11] studied these reactions at 1.15 BeV/c,[9] 1.22 BeV/c, and 1.51 BeV/c.[10,11] Few events were observed at 1.15 BeV/c and the results were not significant. The data at 1.22 BeV/c and 1.51 BeV/c showed strong Y_0^* (1405) and Y_0^* (1520) production. They also observed some enhancement in the 1400 MeV region in the $T_3 = |1|$ system. The enhancement in the data at 1.22 BeV/c was not statistically significant. But the peak is especially sharp in the data at 1.51 BeV/c. The full-width at half-maximum was of the order of 50 MeV. This was explained as due to possible constructive interference between Y_1^* (1385) and Y_1^* (1660) or to ρ meson contamination.

C. $\underline{K^- + n \rightarrow \Sigma^- + \pi^- + \pi^+}$

Alston et al.[11] studied this reaction at a K^- beam momentum of 1.49 BeV/c. They found Y_0^* (1405), Y_0^* (1520), Y_1^* (1660) and possibly some Y_0^* (1815). Y_0^* (1520) dominated the reaction. They concluded that there are no T = 2 resonances below 1900 MeV, although the phase space did not agree very well with the $\Sigma^- \pi^-$ invariant mass distribution. Deviations from their phase space were not insignificant in the 1600 MeV and 1800 MeV regions. There exists some enhancement in the 1450 MeV region but it is within the statistics.

The results of this reaction differs from the results of $K^- + p \rightarrow \Sigma\, 2\pi$ at 1.51 BeV/c discussed above. Y_0^* (1520) dominated both production channels. But Y_1^* (1660) was not needed to explain the data at 1.51 BeV/c. Except for the peak at 1415 MeV in the $T_3 = |1|$ system, the data agrees with the production of only Y_0^* (1405) and Y_0^* (1520).

D. Summary

As can be seen from the foregoing discussion, no T = 2 resonance has been observed. Only one large-statistics experiment has been done with neutrons as target particles. In addition, the K^- momentum range below 1.2 BeV/c has not been studied carefully.

It is well known that the production of resonances can vary greatly with energy. Further, when many resonances are produced in the same reaction, interferences between these resonances can make analysis extremely difficult. Thus, the absence of a T = 2 resonance in previous experiments should not be considered as conclusive evidence that it does not exist.

III. THEORY

A. Global Symmetry with Doublet Approximation[13]

There have been many theories proposed which require the existence of a T = 2 resonance. In general, they are based on similarities between pion-hyperon and pion-nucleon scattering. The oldest of these theories is global symmetry with doublet approximation.

In this theory, one puts the sigmas and the lambda into the form of two doublets to correspond to the two nucleons. These doublets are (Σ^+, Y°) and (Z°, Σ^-) where

$$Y^\circ = \frac{\Lambda - \Sigma^\circ}{2} \qquad Z^\circ = \frac{\Lambda + \Sigma^\circ}{2}$$

The coupling is assumed to be due to pions and it neglects the K-meson contributions. In this way the problem is reduced to the same form as that for the pion-nucleon scattering.

An analogy can be made with the T = 3/2, J = 3/2 pion-nucleon resonance with a mass of 1238 MeV and a full-width of 94 MeV. When extended to the hyperons, the theory predicts two resonances in the pion-hyperon system corresponding to the (3,3) pion-nucleon resonance. The spin of these resonances must be 3/2, the same as that of the (3,3) resonance.

The isotopic-spins, masses, and widths can be obtained approximately in an empirical way. The isotopic-spin $\vec{T}$ is written as the sum of an $\vec{I}$-spin and $\vec{K}$-spin, $\vec{T} = \vec{I} + \vec{K}$. The $\vec{I}$-spin is the isotopic-spin component contributed by the pion alone, whereas the $\vec{K}$-spin is related to the K-meson. It is obvious then, for reactions involving only pions that $\vec{I} = 1$, and $\vec{K} = 0$, but if only kaons are involved, then $\vec{I} = 0$, and $\vec{K} = 1/2$.

We assume the phenomenological mass formula for nucleons and hyperons:

$$M = m(K^2) + \Delta \vec{I} \cdot \vec{K}$$

Here M is the observed mass of a nucleon or a hyperon, $m(K^2)$ is the baryon mass in the absence of pion interaction, and Δ is the mass difference between the sigma and the lambda of approximately 75 MeV.

From the observed masses and the knowledge of $\vec{I} \cdot \vec{K}$, $m(K^2)$ is calculated to be approximately 1171 MeV.

For a resonance between pions and baryons, we must add the pion mass and the total available kinetic energy Q of the resonance. The the mass formula becomes:

$$M = m(K^2) + \Delta \vec{I} \cdot \vec{K} + M_\pi + Q$$

For the special case of the sigma-pion resonance corresponding to the (3,3) pion-nucleon resonance, we have:

$$\vec{I} = 3/2, \ \vec{K} = 1/2 \rightarrow \vec{T} = 2, \ \vec{I} \cdot \vec{K} = 3/4$$

$$M = 1171 + (3/4)\ (75) + 140 + 230 = 1527 \text{ MeV}$$

To obtain an approximate width for the resonance, isotopic-spin weight must be assigned to each final-state channel. This must be further corrected by the differences in available phase space, $(p^*/p^*_N)^{2\ell+1}$, where p^* is the C.M. momentum of the appropriate resonance, p^*_N is the C.M. momentum of the pion-nucleon resonance, and ℓ is the orbital angular momentum of the state considered.

In our case, $p^* = 270$ MeV/c; $p^*_N = 230$ MeV/c; the half-width of the (3,3) resonance is 47 MeV; the (3,3) resonance is a $p_{3/2}$ resonance, therefore, $\ell = 1$. Since the resonance under consideration can decay only into a sigma and a pion, the isotopic-spin weight is 1. So we have:

$$\Gamma/2 = (47)\ (270/230)^3 = 76 \text{ MeV}$$

Thus, the theory predicts a T = 2 sigma-pion resonance with a mass

of 1527 MeV and a half-width of 76 MeV.

B. Limited Symmetry

Essentially these theories are generalizations of the global symmetry theory with doublet approximation. They take into account the difference in couplings between the lambda and the sigma in addition to their mass difference.

As an example, Amati et al.[14] have considered the pion-hyperon scattering using a static meson model analogous to the one pion exchange model for pion-nucleon scattering. The calculation takes into account the two channels, pion-lambda and pion-sigma. In addition, the non-symmetrical coupling and the mass difference of lambda and sigma are introduced.

In this theory, three resonances in each of the two possible J state, 1/2 and 3/2, are allowed. They are in T = 0, T = 1, and T = 2 systems. The interesting observation here is that if the coupling constant $f^2_{\Sigma\Sigma}$ falls to zero, the Y^*_2 predicted in the J = 3/2 system persists and rises in mass value relative to that of the predicted Y^*_1 and resonates at the same mass as the Y^*_0. This mass is 1625 MeV if the mass of the T = 1 resonance is assumed to be 1385 MeV as observed for the Y^*_1 (1385).[15]

It should be noted that the theory reduces to the global symmetry theory when the more limited assumptions of the global symmetry are introduced.

C. SU_3

This is a method of considering the meson-baryon resonances in the hope that some "higher-symmetries" exist. The resonances and particles are grouped into multiplets according to their isotopic spin and hyper-

charge. If this "higher-symmetry" exists, then, in reality it must be broken.

If the symmetry-breaking interaction is assumed to have definite transformation properties, a mass formula can be derived by a first-order perturbation theory calculation.[16] The Hamiltonian is separated into two terms; one is invariant under the group SU_3 and the other transforms in this group like the hypercharge. This separation is unique when possible. The mass formula then gives definite spacings of the masses in the multiplets.

The theory does not predict the existence of a Y_2^*. However, if a Y_2^* exists, it must be in the 27 or higher dimensional representation.

IV. EXPERIMENTAL PROCEDURES

A detailed description of this beam has been published by Eberhard et al.[17] Figure 1 shows the beam layout. The average momentum of the beam was found to be 1.104 ± 0.007 BeV/c at the center of the propane bubble chamber.[18]

During the exposure of this experiment, a magnetic field of 13.5 kilogauss was applied over the 30-inch propane bubble chamber. Approximately 104,000 pairs of stereo pictures were exposed. Only 86,489 frames were used for the actual experiment after pictures of poor quality were rejected.

Two independent methods were used to determine the number of K^- particles.

A. Tau Decays

Since τ decays of K^-, i. e.,

$$K^- \rightarrow \pi^- + \pi^- + \pi^+$$

were unambiguously identifiable on the scan table, the number of K^- in the beam can be accurately determined by finding the number of τ in the pictures. Since the beam momentum (1.104 BeV/c), mean life of K^-, $(1.224 \pm 0.013) \times 10^{-8}$ sec, and the branching ratio for this mode of decay, (5.66%), were all known, we calculated the number of K^- per frame to be 3.47 ± 0.31. This number was obtained from the scanning of 9237 frames of pictures which resulted in 127 tau decays.

B. Delta-ray Production

The cross section of delta rays produced at a given momentum is a function of the velocity of the particle which gives rise to delta rays. Therefore, particles with different masses but with the same momentum

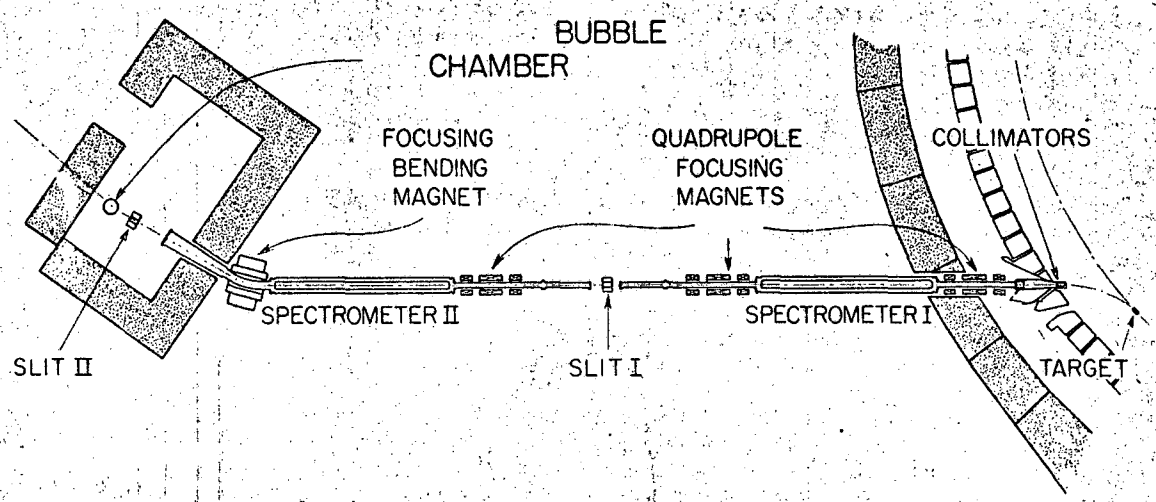

Fig. 1. The experiment layout of the separated K^- beam.

have different cross sections for producing delta rays with a given momentum. At our beam momentum of 1.104 BeV/c, the K^- cannot produce delta rays of kinetic energy above 5 MeV. Consequently, by finding the number of delta rays with a kinetic energy above 5 MeV, we can find the contamination of pions and muons in the beam.

A total of 10,080 chamber lengths of track were looked at. If there were any interactions along the tracks, the lengths were measured up to the point of interaction. A total of 1,125 delta rays of kinetic energy above 5 MeV were found and 37 of these were on tracks which interacted subsequently.

For comparison, we repeated the procedure in a previous 30-inch propane chamber run, where the beam consisted mainly of negative pions at 1.08 BeV/c and had a 10 ± 2% muon contamination.[19] There were, on the average, 24 delta rays and 26.6 interactions per 100 chamber lengths.

When the delta ray counts from the two experiments were compared, the percent of K^- in the beam was calculated to be 56.3 ± 4.5%. Since a muon cannot undergo a significant number of strong interactions, those which did interact were pions. In this way, we separated the pion and muon contaminations. Pion contamination was found to be (11.4 ± 3.2)%; muon contamination was (32.3 ± 3.2)%.

The average number of beam tracks per picture was six. The number of K^-'s per picture was found to be 3.38 ± 0.27.

For cross section calculations, the average of the two independent results was used -- namely, 3.42 ± 0.20 K^-'s per picture.

V. DATA PROCESSING

A. Scanning

The pictures were scanned for sigma production events with one or more visible pions.

The identification of the sigma hyperons depended completely on the ionization change at the point of decay. Thus, a proton which scatters after leaving the carbon atom looks exactly like the positive sigma production followed by the protonic mode of decay. For this reason, we rejected all positive sigmas which decayed via the protonic mode except when there was a definite change in ionization or when one or two gamma pairs were observed to be pointing at the decay point. All sigmas shorter than 3 mm were rejected because of inaccuracies in measurement.

When an event was found, the picture number and the type of event were then written down on the scanning sheet. In one-quarter of the film, all sigmas found were recorded on scan cards. In three-quarters of the film, only those events with two or three pions and zero or one proton were recorded on scan cards.

B. Measuring

The events on scan cards were submitted for measurement on a precision-measuring digitized microscope. Information on the scan card, in addition to locating the event for the measurer, also assigned the event to a definite prescribed category.

The actual measurement, in effect, recorded the coordinates of several points along the measured track with respect to the positions of the fiducial marks on the bottom of the chamber. This was done for both views of the picture. By knowing the positions of the cameras, the

spatial location of the track could be reconstructed.

C. Computer Analysis

The measurements were analyzed by the IBM 7094 through the FOG-CLOUDY-FAIR system.[20]

The FOG program reconstructs each track in space from the separate measurements in the two stereo views of the picture. The momenta are obtained from a parabola fit to the space-reconstructed points for each track except when determined by range measurement. The angles in space are also claculated.

The CLOUDY program performs kinematic constraints in addition to calculating the errors and other quantities of interest, such as invariant mass.

The FAIR program governs the output of information. This may be in the form of page output, tape, histograms, etc.

D. Constraint of Sigma

The pion tracks involved in this experiment were, in general, long and the momenta were well-determined except when the pion left the chamber in a short distance. The momenta of the sigmas were high and the average length was 1.1 cm. Only a minimum value of the momentum could be obtained from range measurement.

Further information can be obtained from the visible decay pion or proton from the sigma. The angle of decay and the pion or proton momentum were used to calculate the momentum of the sigma. This often resulted in solutions which were double-valued corresponding to forward or backward decay of the sigma in the C.M. system. In almost all cases the ionization of the sigma was used to resolve this ambiguity. The range-

momentum relationship was used to find the sigma momentum at the production vertex, but no constraints were applied at this point.

The actual computation was done by the OC constraint in the CLOUDY program used. This is described in the flow chart, Figure 2.

The measurement errors for the tracks in the 30-inch propane chamber have been studied in detail.[20] The errors on the pion momenta involved were of the order of 12%. The angular errors were of the order of one degree. The errors on the sigma momenta were recalculated from the errors on the momenta of the decaying particle and on their decay angles with respect to the sigma direction since the measurement errors were not meaningful. The average error of the sigma momenta calculated after the OC constraint at the decay vertex was approximately 20%.

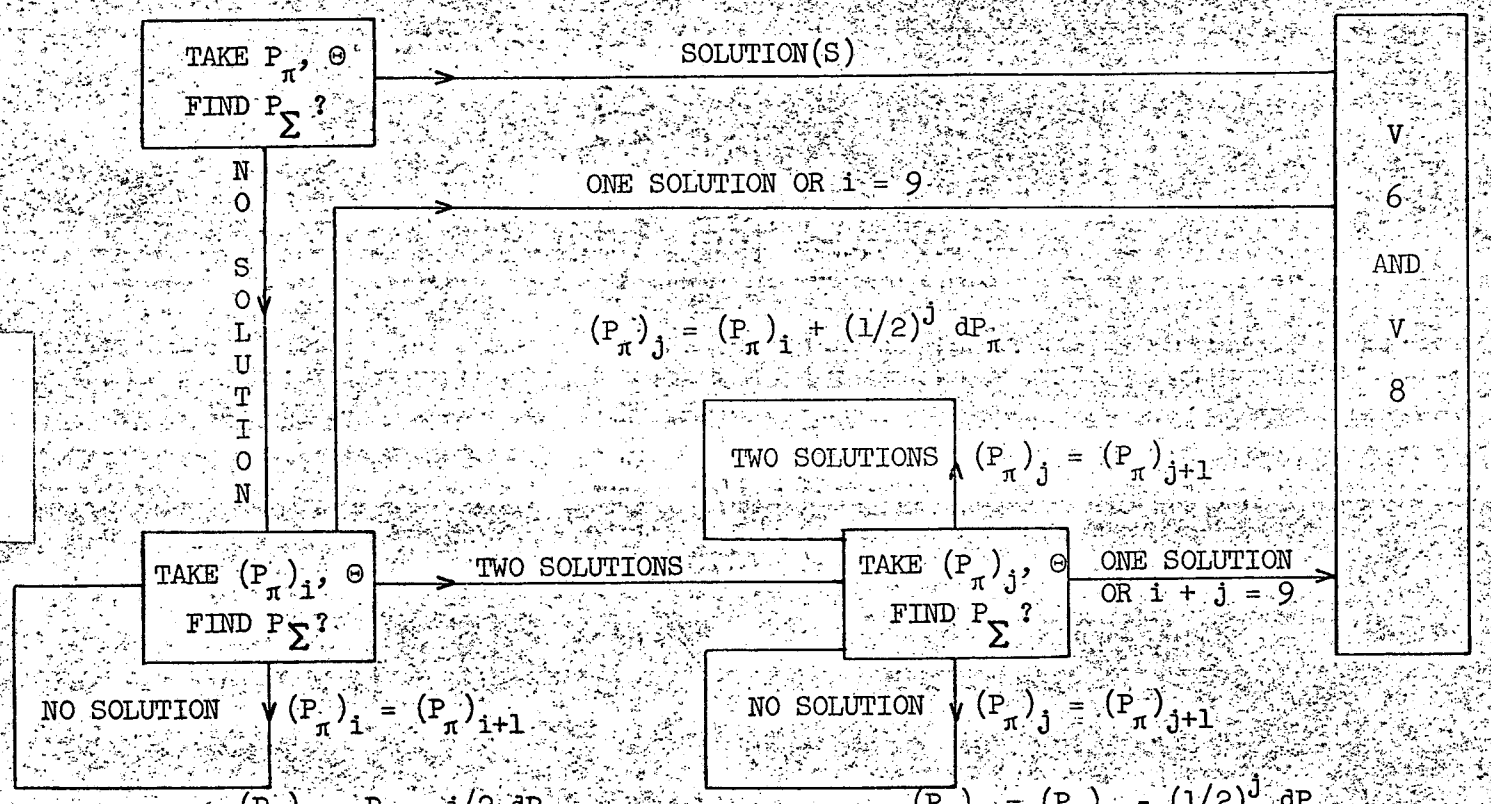
OC CONSTRAINT
TAKE P_π, Θ
FIND P_Σ ?
SOLUTION(S)
NO SOLUTION
ONE SOLUTION OR i = 9
$(P_\pi)_j = (P_\pi)_i + (1/2)^j \, dP_\pi$
V 6 AND V 8
TWO SOLUTIONS
$(P_\pi)_j = (P_\pi)_{j+1}$
TAKE $(P_\pi)_i$, Θ
FIND P_Σ ?
TWO SOLUTIONS
TAKE $(P_\pi)_j$, Θ
FIND P_Σ ?
ONE SOLUTION
OR i + j = 9
NO SOLUTION
$(P_\pi)_i = (P_\pi)_{i+1}$
NO SOLUTION
$(P_\pi)_j = (P_\pi)_{j+1}$
$(P_\pi)_i = P_\pi - i/2 \, dP_\pi$
$(P_\pi)_j = (P_\pi)_i - (1/2)^j \, dP_\pi$
i = 1, . . ., 9
j = 2, . . ., 9
i + j ≤ 9

Fig. 2.

VI. PRELIMINARY CHECKS

A. Lifetime Test for Sigmas

Before the data were analyzed, we checked to see if we were observing real sigmas and to find the number of short sigmas missed in scanning by finding the mean-life of the sigmas.

To do this, we calculated the value of L/P, where L was the total length of the sigma and P was the magnitude of its momentum, for all sigmas with a momenta in the range of 600 to 900 MeV/c. The reason we applied this cut was because calculation showed that the momenta of the sigmas produced with two pions lay in this region. Sigmas with only one visible pion were also used here.

From the exponential decay law, $N = N_0 e^{-t/\tau}$, we see

$$\tau = \frac{t_2 - t_1}{\ln N_1 - \ln N_2}$$

where τ is the mean-life of the sigma; N_1 and N_2 are the number of sigmas found to decay at times t_1 and t_2 respectively. This equation can be expressed in terms of L/P:

$$\tau = \frac{m^2}{Ec}\left[\frac{\frac{L_2}{P} - \frac{L_1}{P}}{\ln N_1 - \ln N_2}\right]$$

The term in the bracket is the slope of the straight line in the lifetime plot, Figures 3 or 4. The straight lines were obtained by a least-square-fit to the data.

From our fits, we found the mean life of the sigma plus to be $0.73 \pm 0.13 \times 10^{-10}$ sec and the mean life of the sigma minus to be $1.12 \pm 0.20 \times 10^{-10}$ sec. These values are to be compared to the quoted values of $0.81^{+0.06}_{-0.05} \times 10^{-10}$ sec and $1.61^{+0.1}_{-0.09} \times 10^{-10}$ sec respectively.

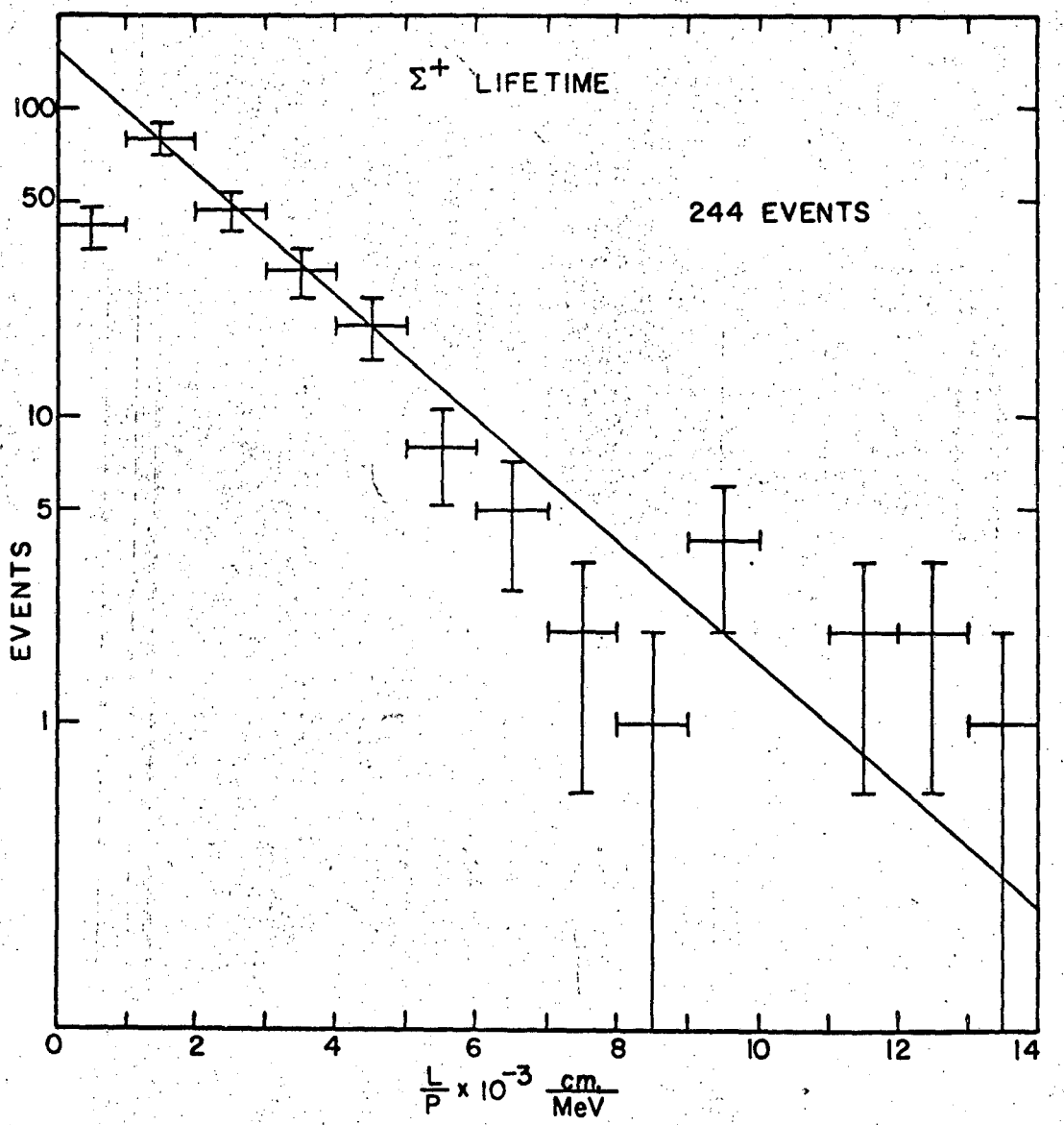

MU-34152

Fig. 3.

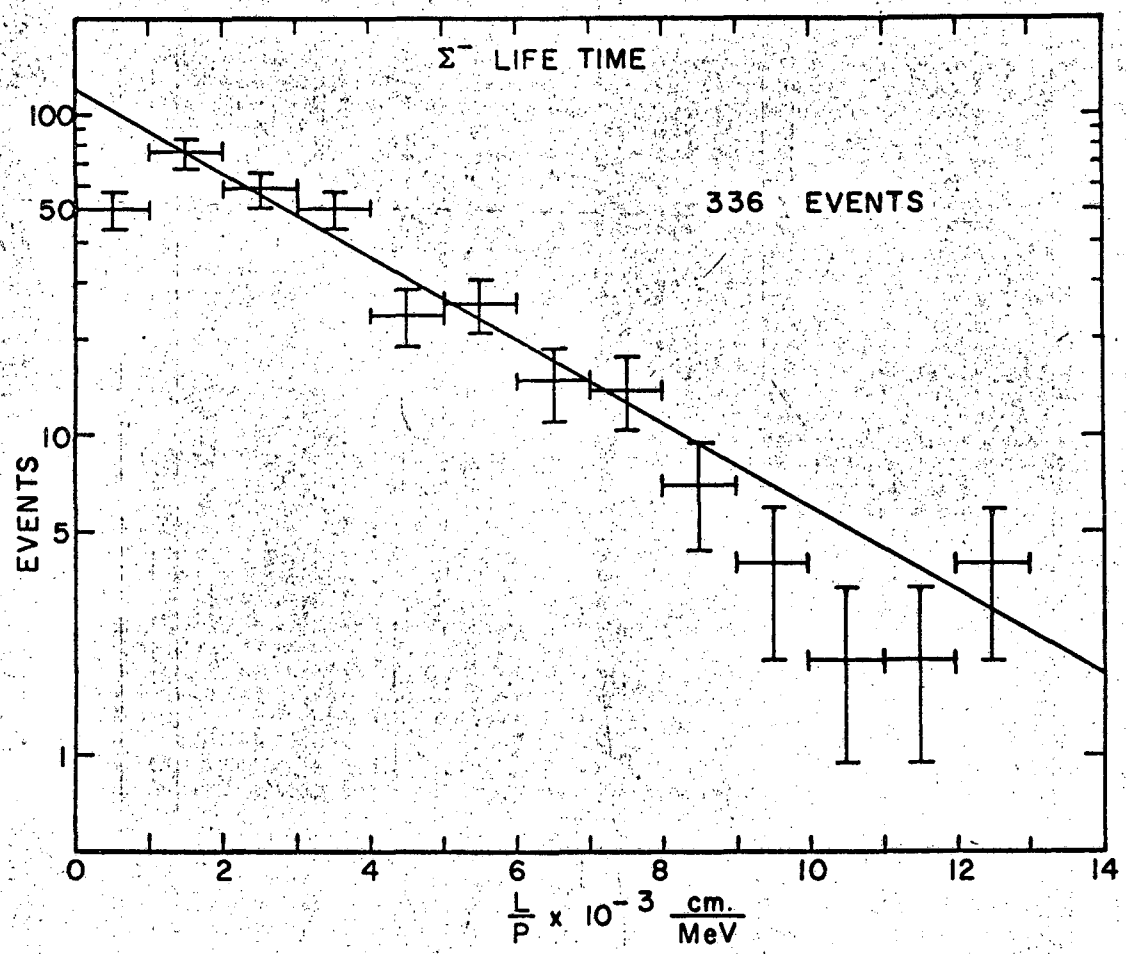

MU-34151

Fig. 4.

In each of the Figures 3 and 4, the first box was not used in the fitting of the data, because each box contained events which were rejected by the 3 mm cut in our scanning. From the deviations from the straight line fits we got 24.4 ± 5.6% missing for positive sigmas and 13.2 ± 5% events missing for negative sigmas. Note that the ratio of the missing events in the first box for sigma plus to sigma minus is approximately two. This reflects the one-half factor in the life times.

Sigmas of lower and higher momenta gave similar results.

B. Scanning Bias Test

Detection efficiency decreases when the track in the bubble chamber goes toward or away from the cameras. To check this bias, we looked at the azimuthal angle distribution of the outgoing particle with respect to the incoming particle. The azimuthal angle, Φ, is zero degrees when the outgoing particle goes toward the cameras, (upward in the chamber), and 180 degrees when it goes away from the cameras, (downward in the chamber). The azimuthal angle distribution should be isotropic if there were no bias.

Two azimuthal angles were involved. The first was the one the sigma made with the incoming K^-. The second was the one the decay particle of the sigma made with the sigma direction.

The distribution at the production vertex, Figure 5, is isotropic within statistics. Figure 6 shows a twice-folded plot of the events against Φ for the decay pions. There is a marked bias against those pion tracks going toward or away from the cameras. As a result of this bias, approximately 25 ± 2% of the events were lost.

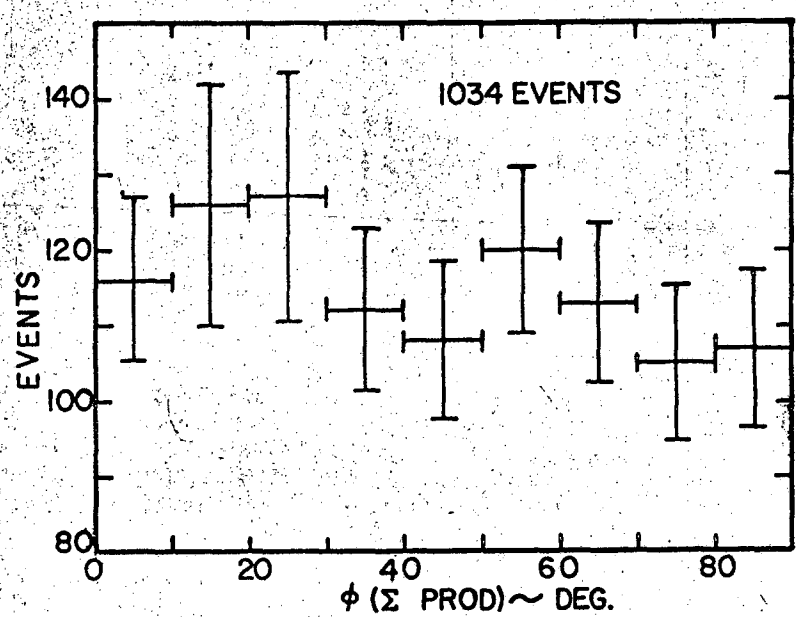

MU-34155

Fig. 5.

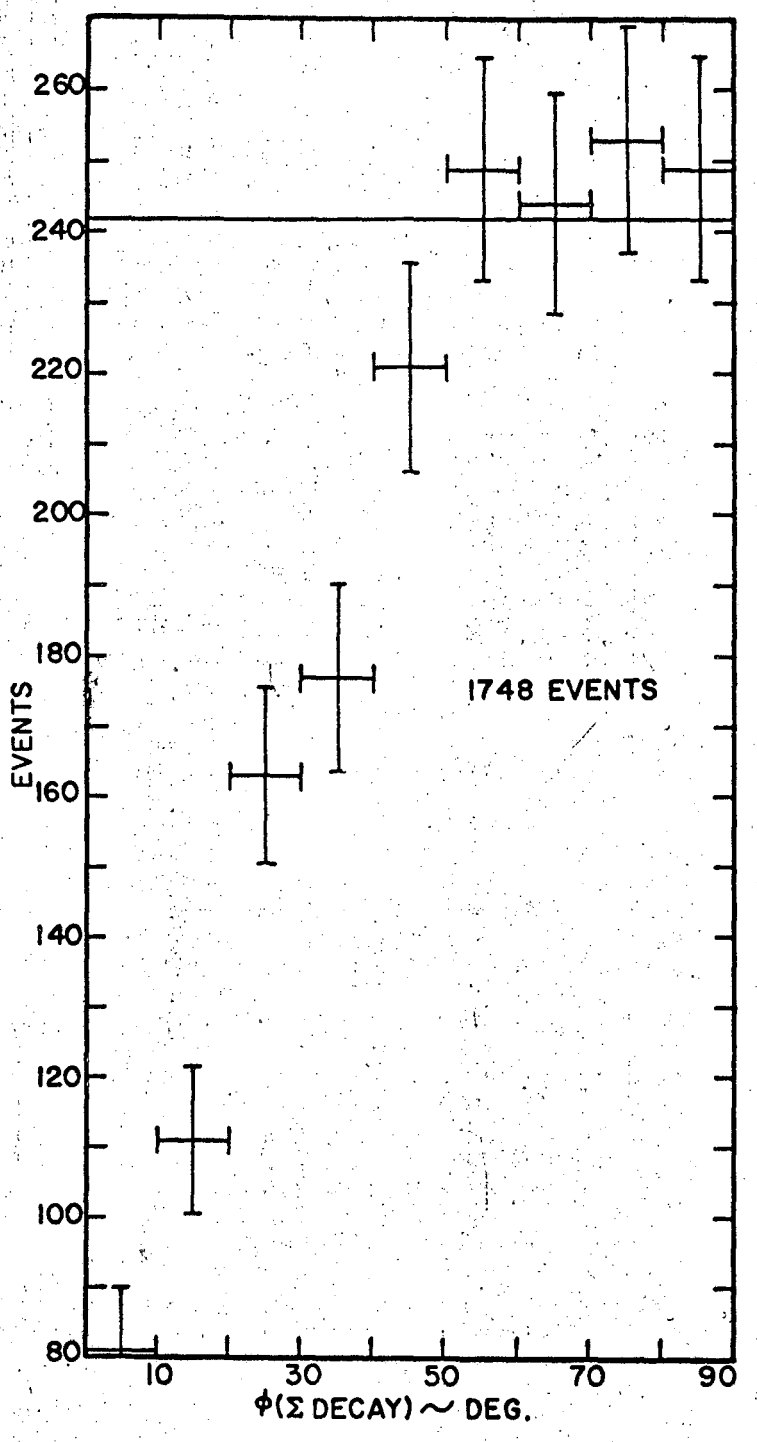

MU-34156

Fig. 6.

C. Scanning Efficiency Determination

To find the number of events missed in the scanning, approximately one-third of the total "good" film was scanned independently by two different scanners. The scanning efficiency of any one scanner could then be found from the formula

$$e_i = \frac{N_{ij}}{N_{ij} + n_j}$$

where N_{ij} is the number of events found by both scanner i and j, and n_j is the number of events found by scanner j and missed by i. Assuming that the scanning efficiency of the scanner stayed constant, the total number of events in the film scanned by the scanner is just the ratio of the events actually found by the scanner i and his efficiency, i.e., N_i/e_i.

The over-all average scanning efficiency for this experiment was found to be 89.7 ± 6% for the sigma-two-pion events.

VII. PRODUCTION CROSS SECTION

In order to calculate the cross section for the sigma-two-pion production on neutrons, it was necessary to know the total beam path length. The fiducial volume was defined in such a way that the interaction length was 40 cm. But because of interactions, the average path length per beam kaon had to be calculated from known mean-free path length for kaons. This was computed, from the K-nucleon total cross sections,[21] to be 159 ± 11 cm. From the formula

$$L = (\lambda)\,(1 - e^{-\frac{\ell}{\lambda}})$$

where ℓ is the interaction length and λ is the mean-free path length, we found the average path length per beam kaon to be 35.3 ± 2.5 cm. After multiplying the total frames scanned and the average number of kaons per picture by the average path length per beam kaon, we found the total kaon track length in this experiment to be $10.44 \pm 0.95 \times 10^6$ cm.

The sigma plus cross section was based on the events where the Σ^+ decayed into a π^+ and a neutron. It was then multiplied by two to take care of the protonic decay mode which was eliminated from the cross section determination. At the production point, the zero and one proton events were added together because the protons were assumed to be just recoils and not associated with the sigma production events. All the data were added in this fashion.

The density of propane used in the cross section calculations for the sigma-two-pion events was 0.415 gm/cm^3. The summary of the scanning results and the cross sections, along with the corrections made, is presented in Tables 1 and 2.

TABLE I

Type of Event	Number Found in Scanning	Number on Output	Number with Difficulties in Measurement	Number Rejected as Not Sigma
$\Sigma^- \pi^- \pi^+$	237	217	5	9
$\Sigma^- \pi^- \pi^+ p$	93	75	8	6
$\Sigma^+ \pi^- \pi^-$	127	105	3	18
$\Sigma^+ \pi^- \pi^- p$	53	47	-	4

TABLE II

Type of Event	Found (Corrected)	Total Observed	Life-Time Correction	Decay Bias 25 ± 2%	Scanning Efficiency 89.7 ± 6%	Total Corrected	Cross Section
$\Sigma^- \pi^- \pi^+$	228	315	13.2 ± 5%	484	540	540	0.51
$\Sigma^- \pi^- \pi^+ p$	87		363				± 0.07 mb
$\Sigma^+_\pi \pi^- \pi^-$	85	123	24.2 ± 5.6%	216	241	(241) (2)	0.45
$\Sigma^+_\pi \pi^- \pi^- p$	38		162			482	± 0.07 mb

VIII. PHASE SPACE AND RESOLUTION

A. Phase Space

The standard method of looking for resonances in an n-body system is to look for deviation from phase space in the invariant mass plot. The invariant mass of an n-particle system is defined as

$$M_n = \left[\left(\sum_{i=1}^{n} E_i\right)^2 - \left(\sum_{i=1}^{n} \vec{P}_i\right)^2 \right]^{1/2}$$

When many resonances exist in the same energy region, a resonance in one invariant mass can be obscured by the reflection of another. Alternatively, one can look for clustering of events on a Dalitz plot.

A Dalitz plot is a scatter-diagram of the appropriate quantities from which one can deduce the constancy of the square of the matrix element for the reaction. In the absence of any resonance, i.e., constant or slowly varying matrix element, the points representing the events should be populated uniformly on the plot. The limit of the Dalitz plot is governed by the available energy.

In collisions with single nucleons, the total energy of the outgoing particles is fixed by the beam momentum. In our case, the carbon nucleus can take some energy which may be unobserved. The appropriate Dalitz plot uses the square of the invariant mass of the sigma-pion system. This still preserves the property that every element of area has equal à priori probability of being occupied, and at the same time allows all the events with the same mass of the sigma-pion system to fall on the same line. The alternative of using C.M. kinetic energies of the two pions is not suitable here because of our inability to transform the laboratory quantities into the C.M. system properly.

In our case, we had a variable C.M. energy available because of the Fermi momentum of the nucleon in the carbon nucleus. The phase space and the boundary of the Dalitz plot are no longer defined by the beam momentum. To calculate the total phase space, we adopted the following procedure:

1) The invariant mass of the total three-body system was calculated for each event. This was the available energy in the C.M. for the three-body system.

2) The standard three-body phase space was calculated for each event corresponding to the C. M. energy available to the system.

3) All the phase space distributions calculated for each event were then added. Each distribution was given the same weight in the summation.

B. Resolution

The two weighted histograms of the errors in the invariant masses are shown in Figures 7 and 8. The resolution is the half-width at half-maximum of the error histogram. The resolution was 16 MeV for the sigma-pion invariant mass and 8 MeV for the pion-pion invariant mass.

It should be pointed out here that the resolution obtained for the sigma-pion invariant mass was an average. It was noticed that the errors were directly proportional to the magnitudes of the invariant mass.

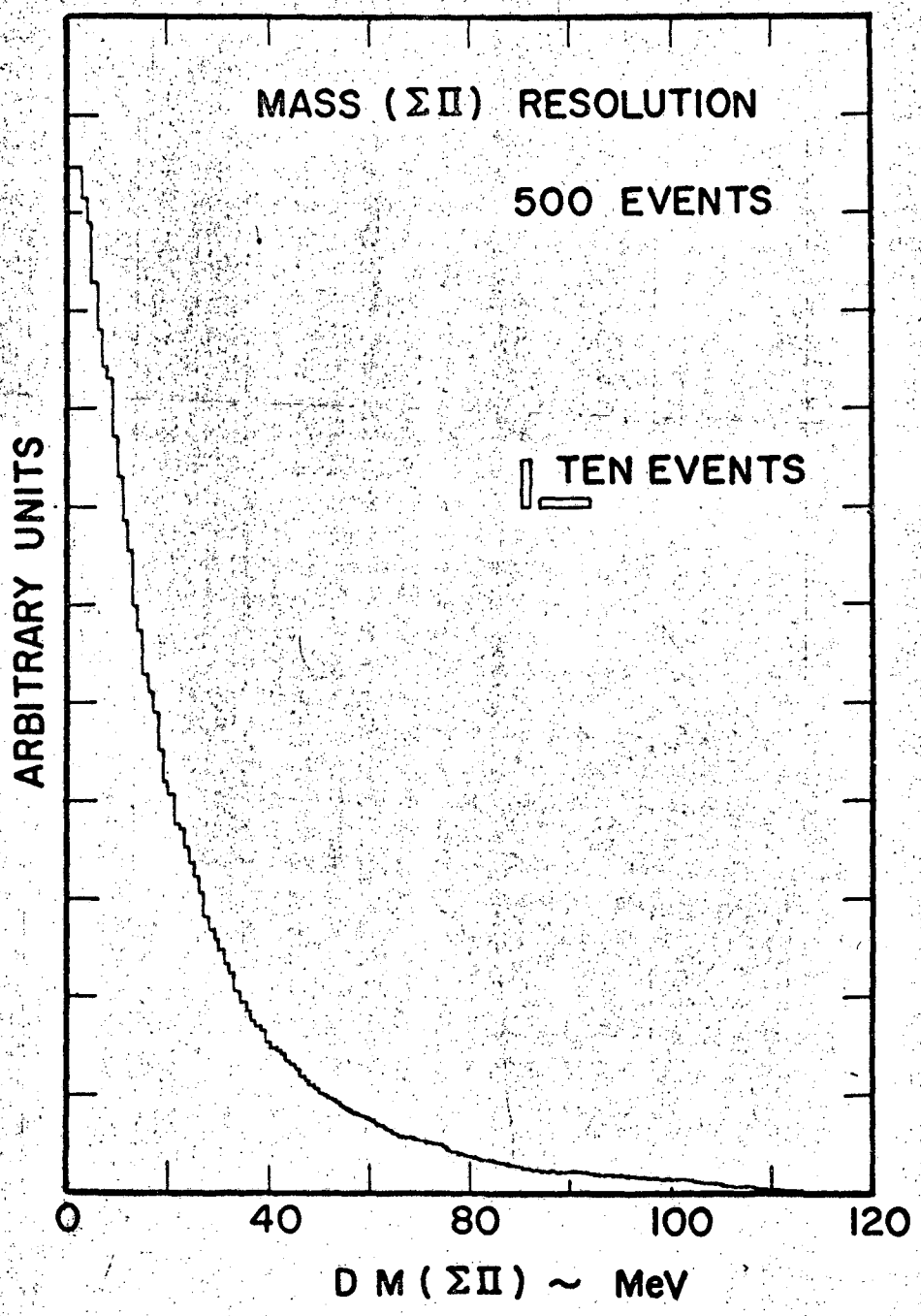

MU-34154

Fig. 7.

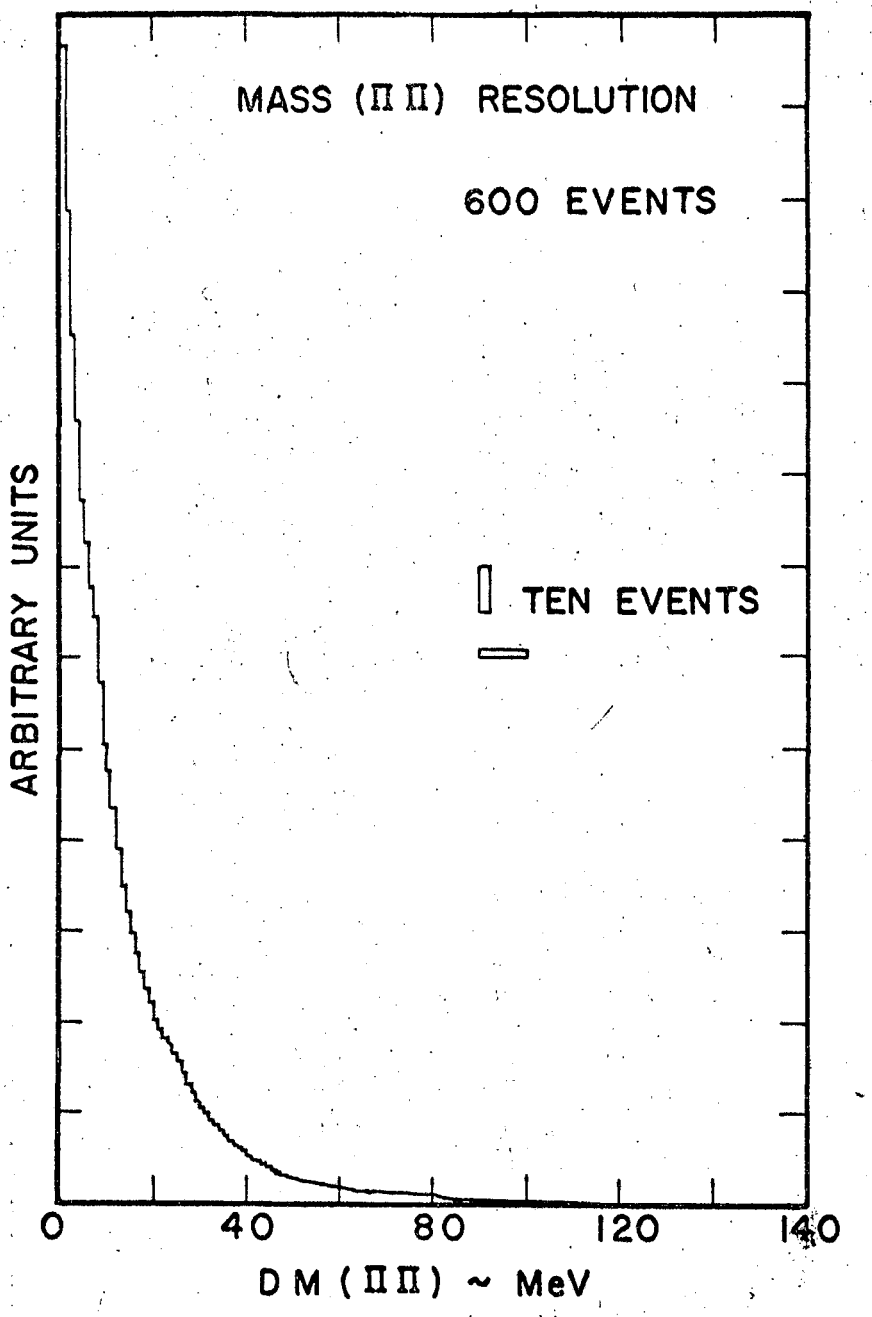

MU-34153

Fig. 8.

IX. RESULTS AND DISCUSSION

In this section we will consider the nucleon Fermi momentum in carbon. Then we will discuss resonances in the three- and two-body invariant mass systems.

A. Fermi Momentum Distribution

To check if our data is consistent with single neutron interaction in carbon hypothesis, we plotted the transverse momentum imbalance of the out-going $\sum 2\pi$ system. This imbalance is independent of the beam momentum. Only $\sum 2\pi$ events with no protons were used. In order to minimize the errors on the transverse momentum imbalance, those events with all the pions greater or equal to 10 cm in length were used exclusively. The distribution is shown in Figure 9. There were 12 events with momenta greater than 600 MeV/c.

The nucleon Fermi momentum distribution in carbon had been measured by Azhgirey et al.[23] using protons with an energy of 660 MeV as incident particles. Their data was fitted by a sum of two Gaussian distributions:

$$\exp\left(-p^2/s_1^2\right) + \alpha \exp\left(-p^2/s_2^2\right)$$

where $\alpha = 0.09$; $s_1^2 / 2m = 16$ MeV; $s_2^2 / 2m = 50$ MeV; p is the momentum and m is the mass of the nucleon in carbon. We used the same fit. The distribution is not normalized in Figure 9. The agreement is excellent. This indicates that it is reasonable to assume that the production of the $\sum 2\pi$ events took place on a single neutron in carbon.

B. Y-2π System

We followed the procedure outlined and calculated the three-particle invariant masses for the lambda and sigma two-pion events.

The distributions are shown in Figures 10 and 11. In the plots,

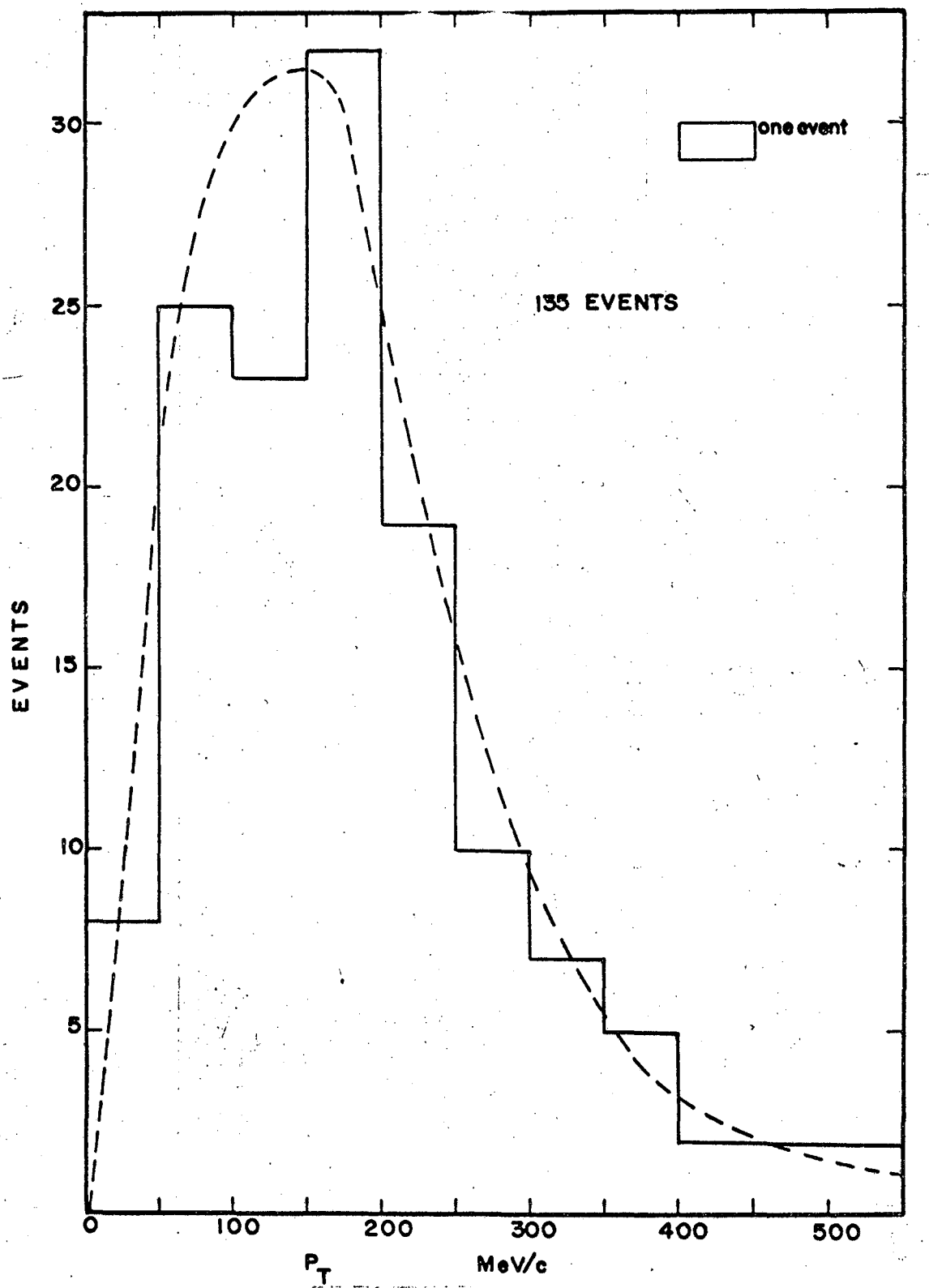

Fig. 9.

MU-34387

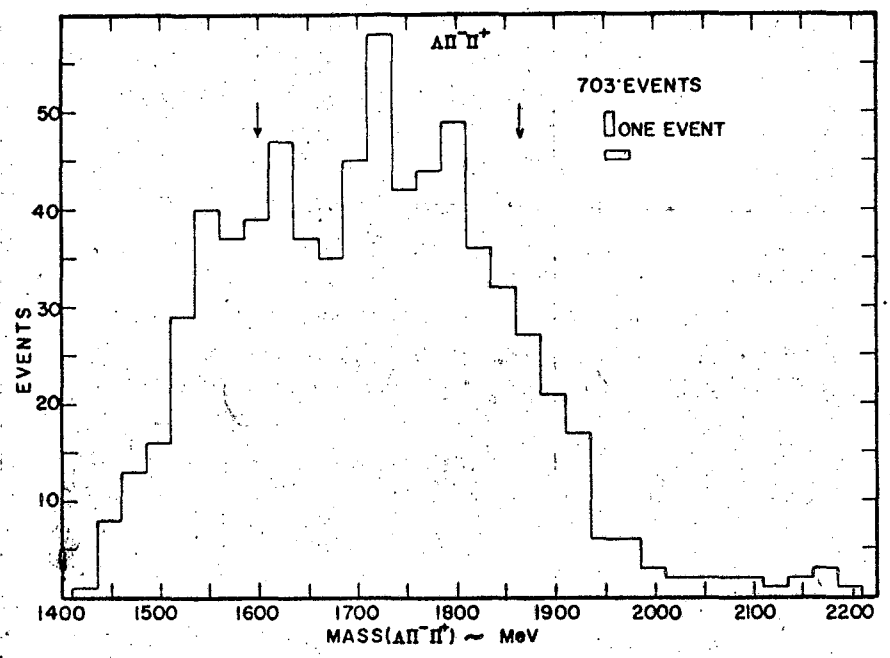

MU-34159

Fig. 10.

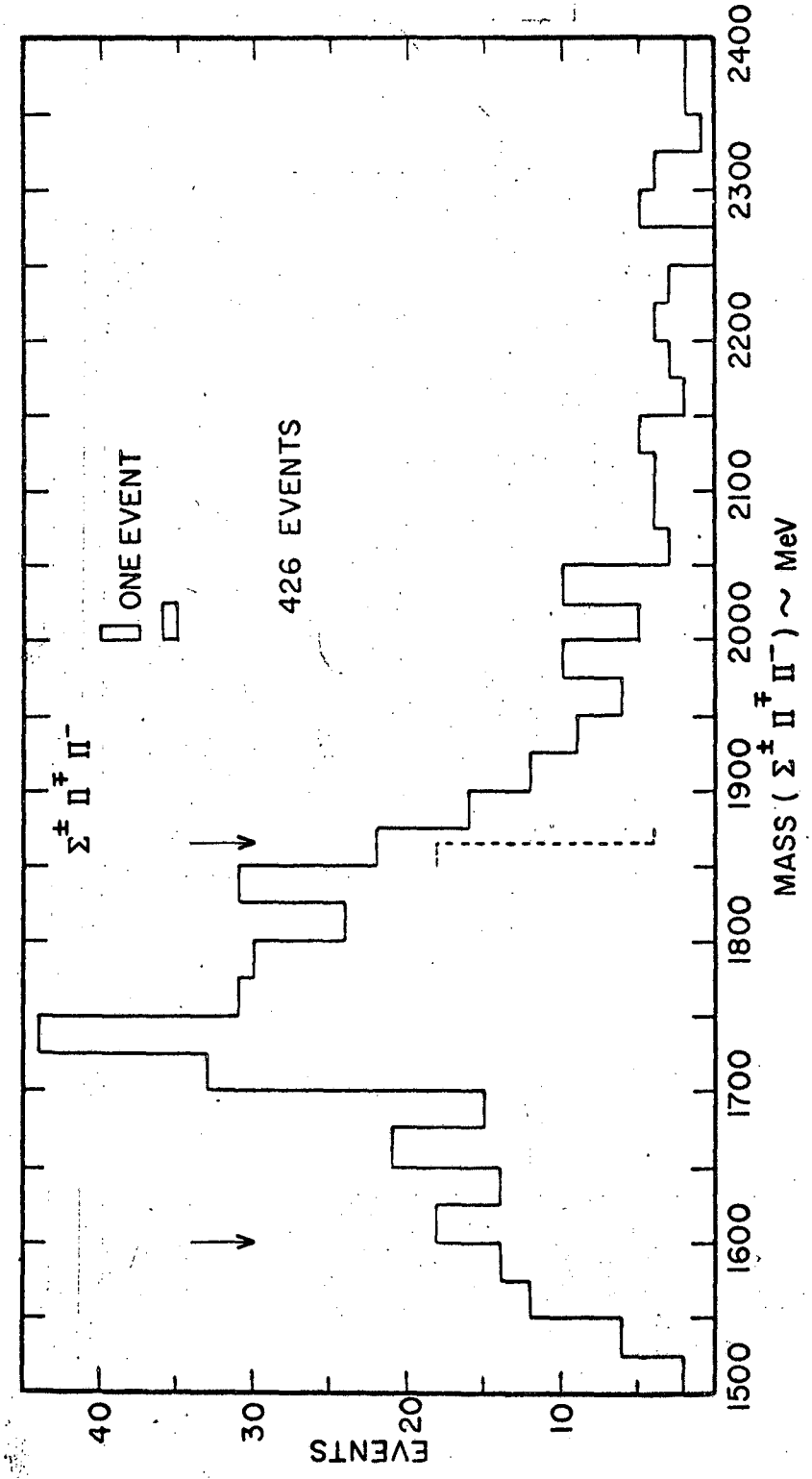

MU-34136

Fig. 11.

we noted the appearance of some enhancement in the 1750 MeV region. This is the area where Tripp et al.[2] observed a bump in the KN scattering cross section corresponding to a resonance which has an isotopic spin of 1. We believe this effect is not due to statistical fluctuations or to the effects of scattering on carbon nucleus. This enhancement may be due to the resonance noted.

C. Lambda-two-pion Events

As a first step in our search for sigma pion resonances, it is necessary to show that similar resonances can be produced in carbon and analyzed. Since the neutrons are bound in carbon, we must show that the proposed method of calculating phase space is reasonable. To do this, we decided to look for the well-known Y_1^* (1385) in our lambda data.

The lambda events were a by-product of a previous experiment concerned with Y_1^* (1385).[22] The accepted events for analysis were such that they satisfied the following criteria:

1) The events constrained as lambdas at the decay vertices (see Figure 3, Reference 22).

2) The events were constrained as interactions on free protons. When the chi square of the fit was 12 or lower, the events were accepted as free proton interactions. If $\Sigma^\circ \pi^- \pi^+$ events were constrained as $\Lambda \pi^- \pi^+$, the chi square of the fit would peak at a value of 25. We accepted only events where the chi square of the fit was above 50. (See Figure 4, Reference 22.)

From Figure 10 we see that there is a wide variation in the C.M. energy available to the lambda-two-pion system. To obtain a reasonable sample of events for further analysis, we selected only those events

with $\Lambda\ \pi^-\ \pi^+$ invariant mass between 1600 and 1865 MeV. The lower cut was determined by the phase space available for the production of the Y_1^*, and the upper cut was the available C.M. energy in the absence of nuclear Fermi momentum.

The two-body phase spaces for the 391 remaining events were calculated following the prescribed procedure. The mass value used for the Y_1^* in the calculation was 1378 MeV as found in our own hydrogen data. The width used was the standard 50 MeV, although our own data showed the widths to be different for the Y_1^{*+} and Y_1^{*-}; the widths being 58 MeV and 70 MeV respectively.[22] The calculated "carbon" phase spaces are shown in Figure 12.

The invariant mass distributions for the lambda-pion systems are shown in Figure 13. The chi-square probability for a worse fit to the non-resonating phase space was less than 5% for the $\Lambda\ \pi^+$ distribution and 1% for the $\Lambda\ \pi^-$ invariant mass distribution. The existence of Y_1^{*-} (1385) is clear, indicating that resonances produced in carbon can be observed. The Y_1^{*+} (1385) is known to be suppressed in this energy region by a factor of 1.5 relative to the Y_1^{*-} (1385).[22] The data was roughly fitted when the phase space was weighted by 115 Y_1^{*-}, 35 Y_1^{*+}, and 241 background. The chi-square obtained for the $\Lambda\ \pi^+$ and $\Lambda\ \pi^-$ distributions gave a 20% and 60% probability, respectively, for a worse fit. The number of Y_1^* used in the fit should not be taken too seriously because of the large interference effects known to exist in this energy region.[24] It is quite obvious that the peaks in the $\Lambda\ \pi^+$ and $\Lambda\ \pi^-$ invariant mass plots have different central values. This is true to some extent even in our hydrogen data.[22] In addition, our hydrogen data gave

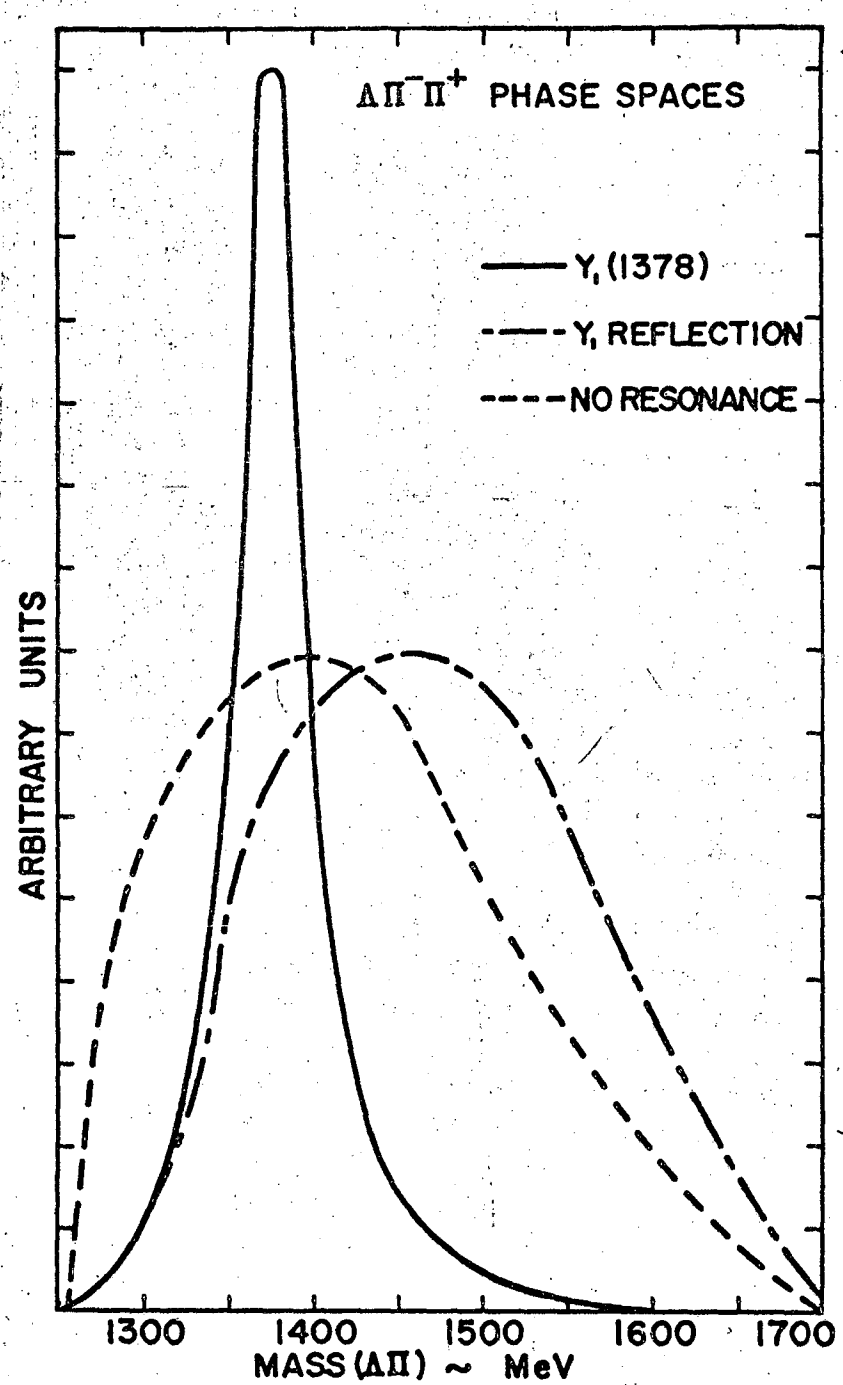

MU-34147

Fig. 12.

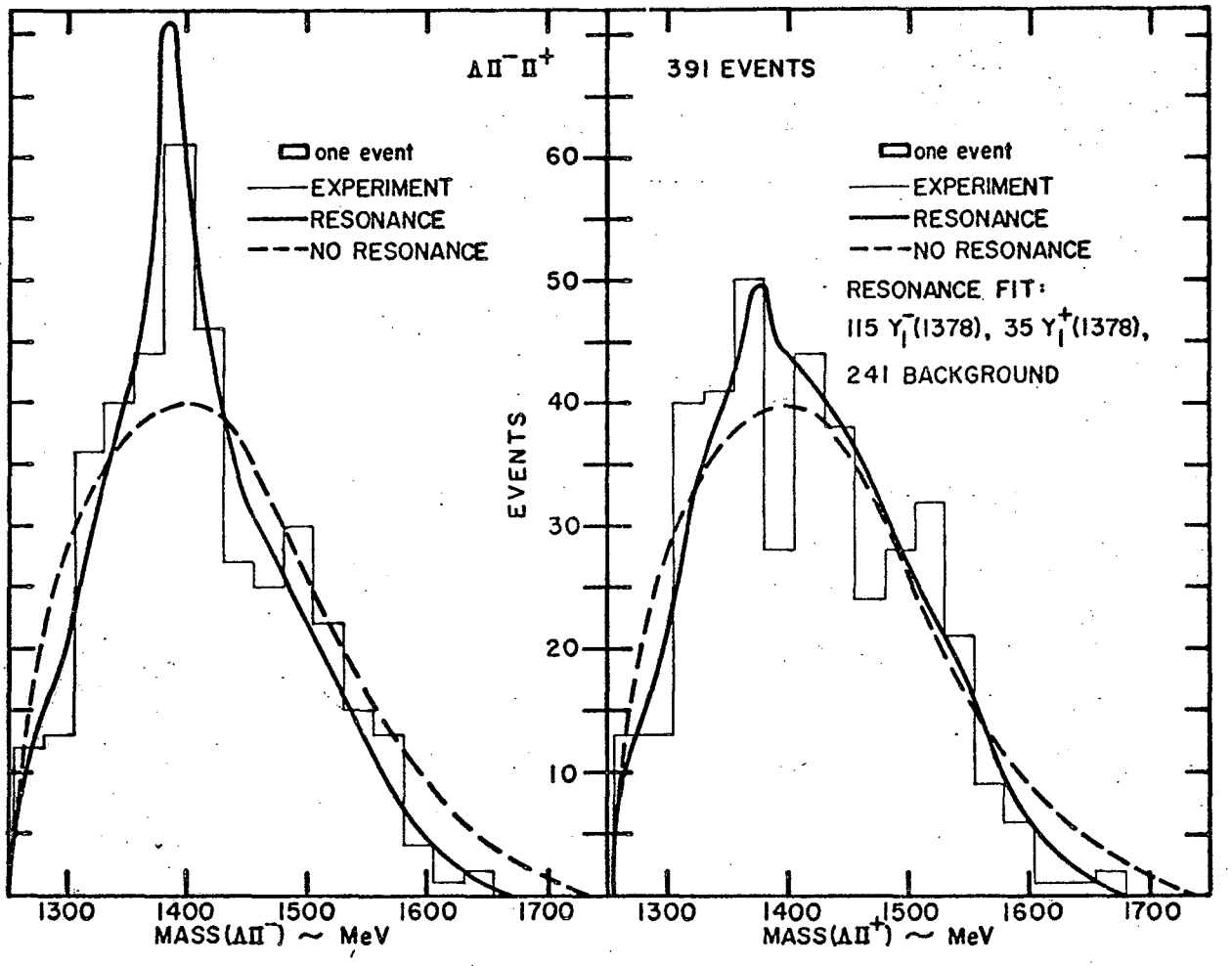

MU-34149

Fig. 13.

wider widths for Y_1^{*-} and Y_1^{*+}. Thus, it is clear that if we used different mass values and different widths for Y_1^{*-} and Y_1^{*+}, we would have gotten more Y_1^* production in our fit.

No peaking was observed in the $\pi^- \pi^+$ invariant mass distribution.

D. $\Sigma^+ \pi^- \pi^-$ Events

We took the same C.M. energy cuts for the sigmas as for the lambdas. The phase spaces calculated in the prescribed manner are shown in Figures 14 and 15. The masses and widths used in the calculations were: 1405 MeV, 50 MeV; 1520 MeV, 16 MeV. These are the best known values for these resonances.

Figure 16 shows the Dalitz plot for the events. The different ellipses are the kinematical limits for several available energies. In the $\Sigma^+ \pi^-$ invariant mass plot, Figure 17, each event was entered twice because of the two negative pions. The probability for a worse fit to the non-resonating phase space was approximately 3%, while the probability for a worse fit to the phase space with resonances was 45%. The phase space with resonance contain 26 Y_0^* (1405), 18 Y_0^* (1520), and 50 non-resonating background. The dominating resonance is clearly the Y_0^* (1520). But it appears to be somewhat lower and broader than the values used in the phase space calculation. The same lower and broader values were observed by Alston et al. in their data at $P_{K^-} = 1.49$ BeV/c.[11]

Figure 18 shows the invariant mass distribution of the negative pions. There are no well-established T = 2 pion-pion resonances in our energy region. There are no statistically significant peaks in our plot. A pion-pion resonance would result in a cluster of events about a diagonal line with slope equal to -1 in the Dalitz plot, Figure 16.

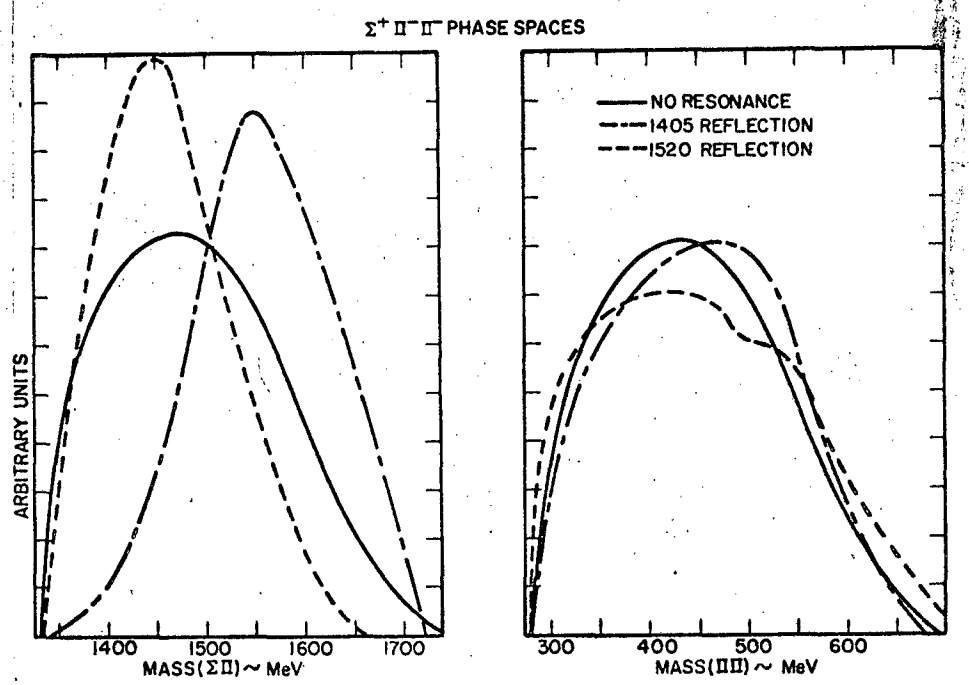

MU-34158

Fig. 14.

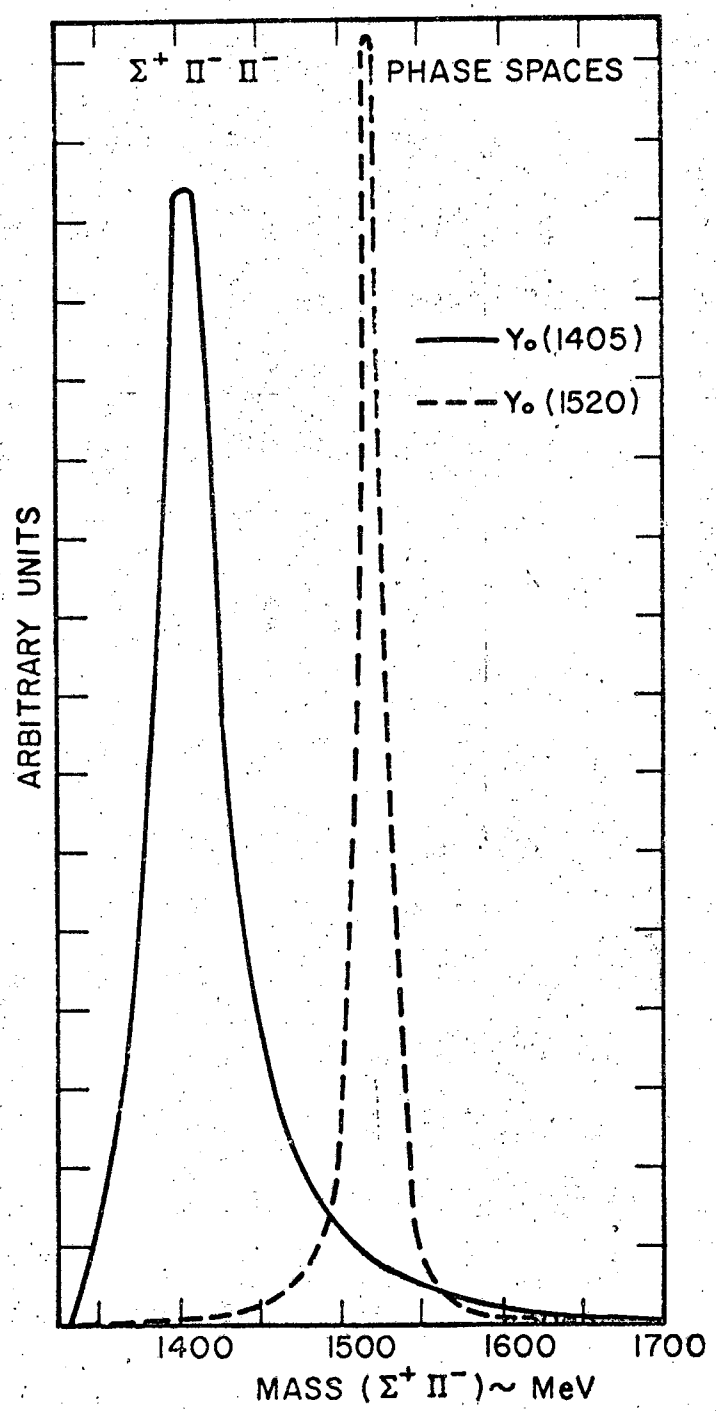

Fig. 15.

MU-34141

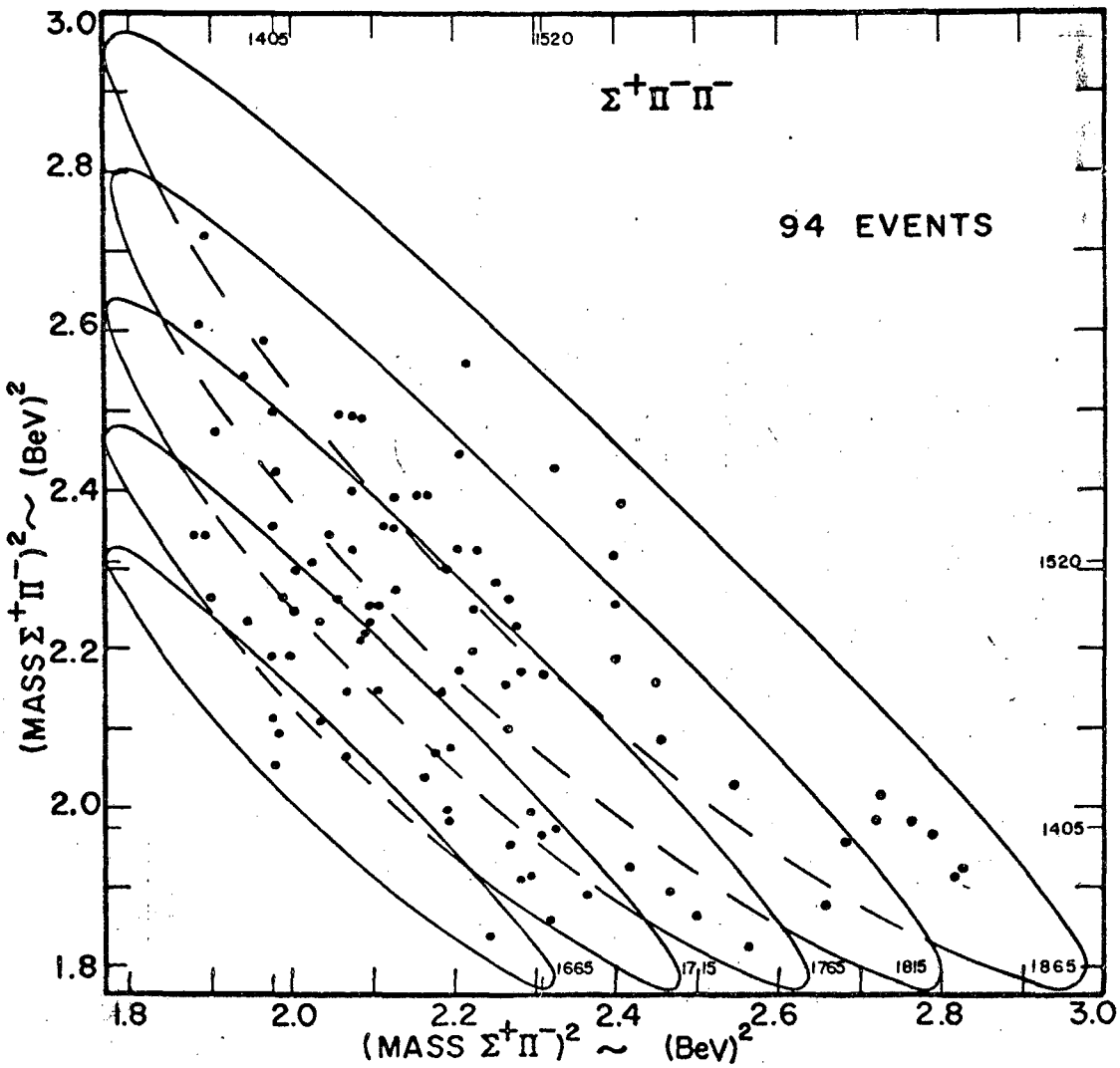

MU-34144

Fig. 16.

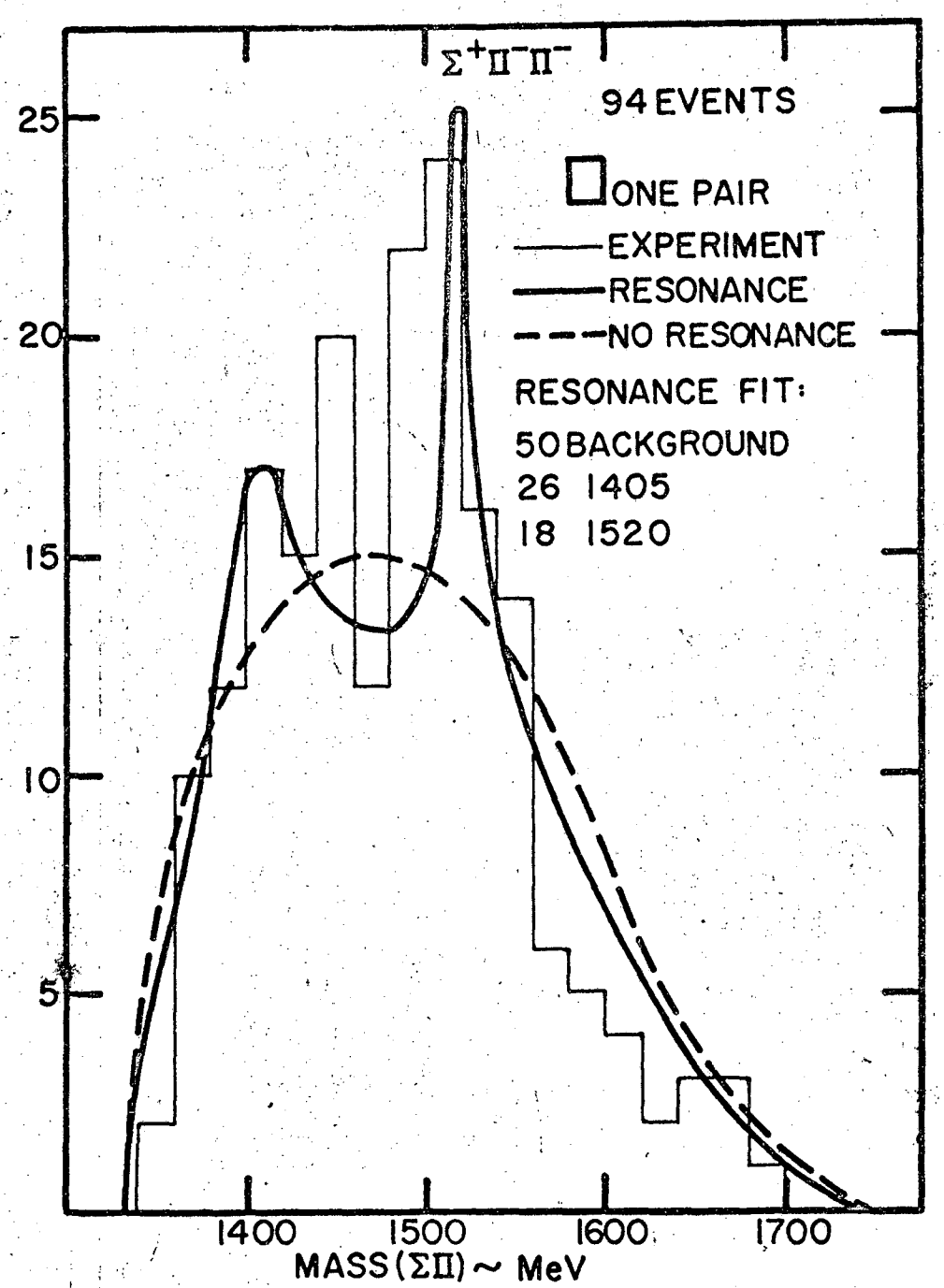

MU-34161

Fig. 17.

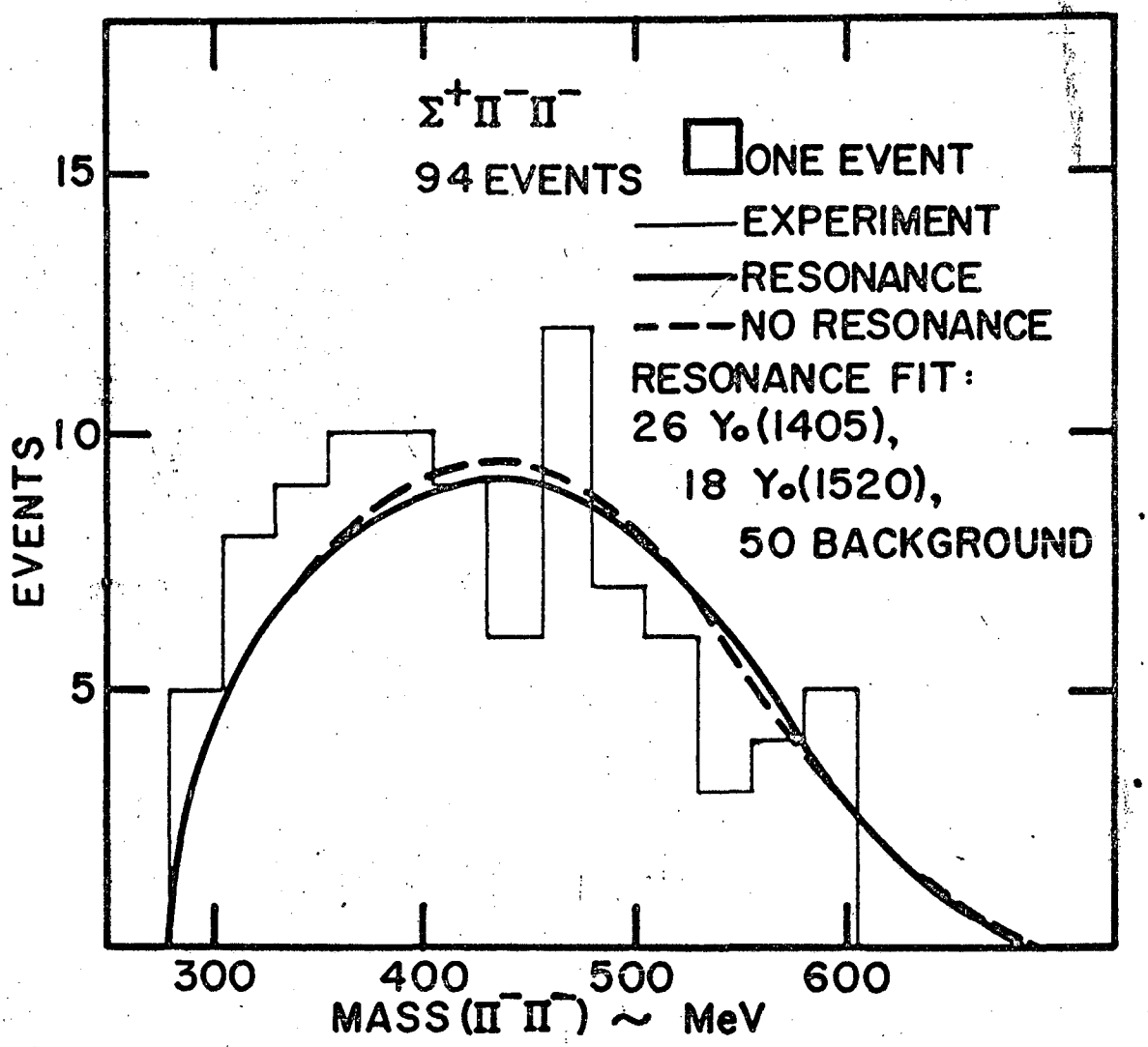

MU-34148

Fig. 18.

We see no evidence for a pi-pi resonance.

E. $\Sigma^- \pi^- \pi^+$ Events

1) Discussion

Following again the procedure outlined above, the phase spaces were calculated. They are shown in Figures 19 and 20. In the $\Sigma^- \pi^+$ invariant mass distribution plotted in Figure 21, we see the familiar Y_0^* (1405) and an indication of the Y_0^* (1520). But unlike the sigma plus events, the Y_0^* (1405) is clearly the dominant resonance here. The chi-square probability for obtaining a worse fit to the non-resonating phase space was 20% and 10% respectively for the $\Sigma^- \pi^+$ and $\Sigma^- \pi^-$ invariant mass distributions.[25] The probability for a worse fit to the phase space with resonance was 50% for the $\Sigma^- \pi^+$ distribution and 90% for the $\Sigma^- \pi^-$ distribution. The phase space with resonances was weighted by 46 Y_2^{*--} (1405), 35 Y_0^* (1405), 10 Y_0^* (1520), and 94 background. The $\pi^- \pi^+$ invariant mass distribution shows nothing out of the ordinary, (Figure 22). The resonance fits were all approximate.

The strong enhancement observed at 1415 MeV in the $\Sigma^- \pi^-$ invariant mass plot in Figure 23 is less than 50 MeV wide. A comparison with Figure 19 shows that the reflection of the Y_0^* (1405) or Y_0^* (1520) cannot give this sharp peak. For example, the width at half-maximum of the Y_0^* (1520) reflection is approximately 70 MeV. And on the Dalitz plot (Figure 24) we see that there is comparatively sparse clustering in the $T_3 = 0$ system at 1405 or 1520 MeV. The main bunching is located at an invariant mass squared value of approximately 2 $(\text{BeV})^2$ in the $T_3 = -2$ system. Thus, the 1415 enhancement is not due to reflections of Y_0^* (1405), Y_0^* (1520) or pion-pion resonances. A comparison with the $\Sigma^+ \pi^-$

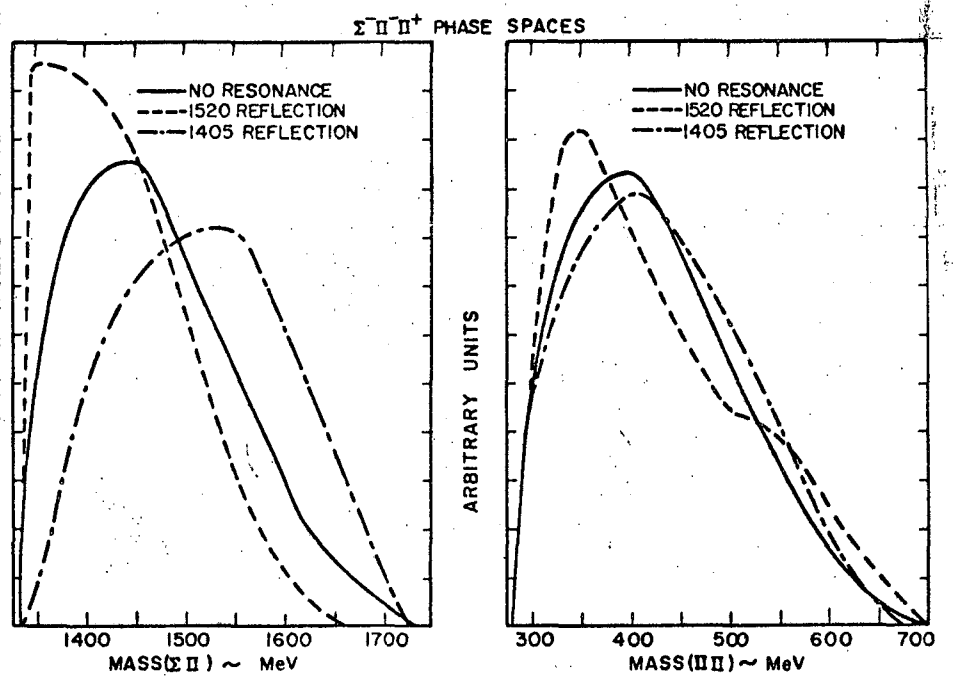

MU-34157

Fig. 19.

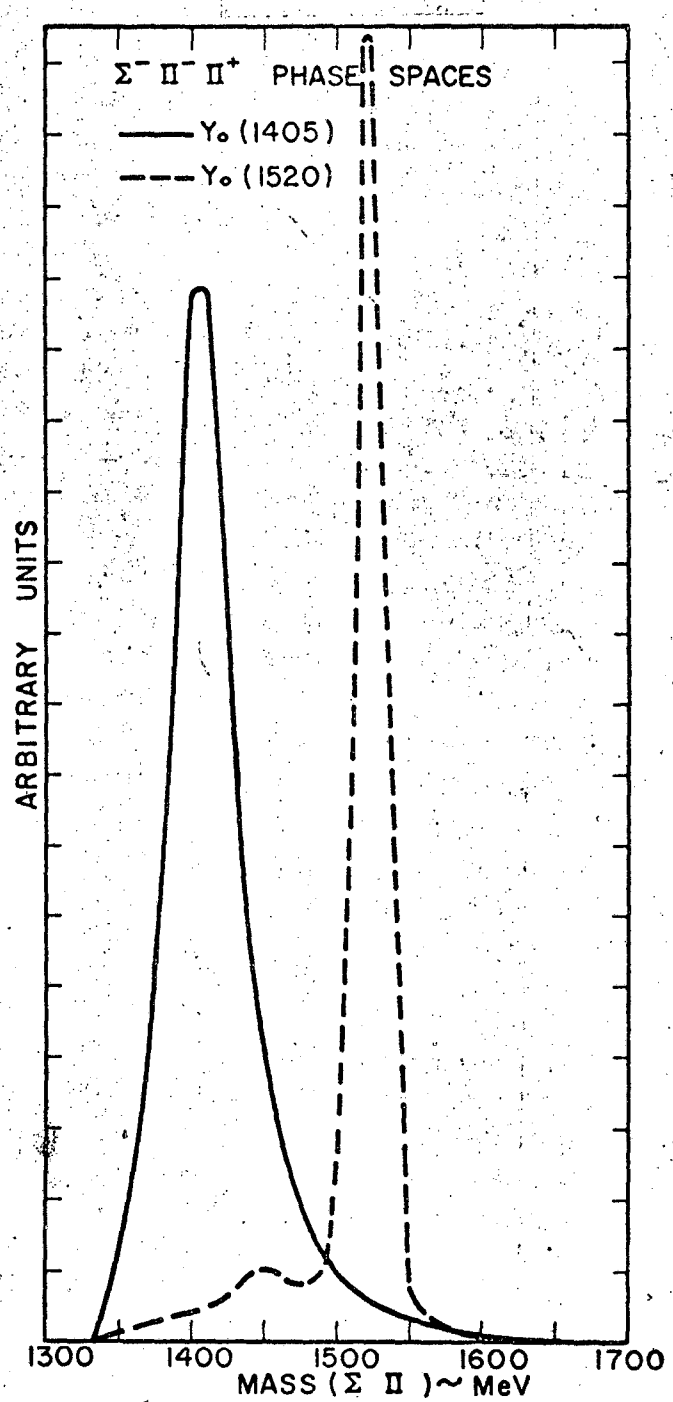

MU-34137

Fig. 20.

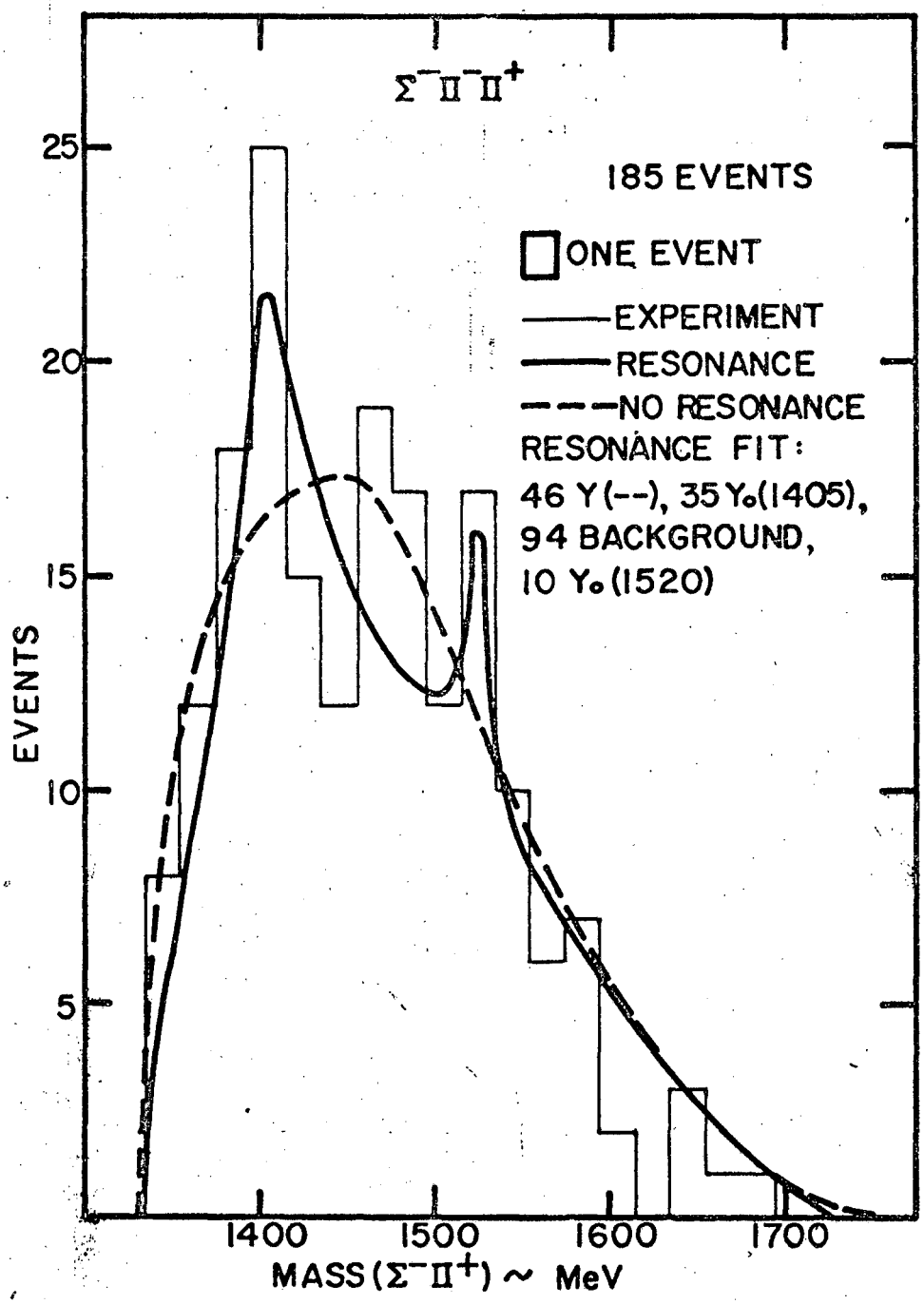

MU-34166

Fig. 21.

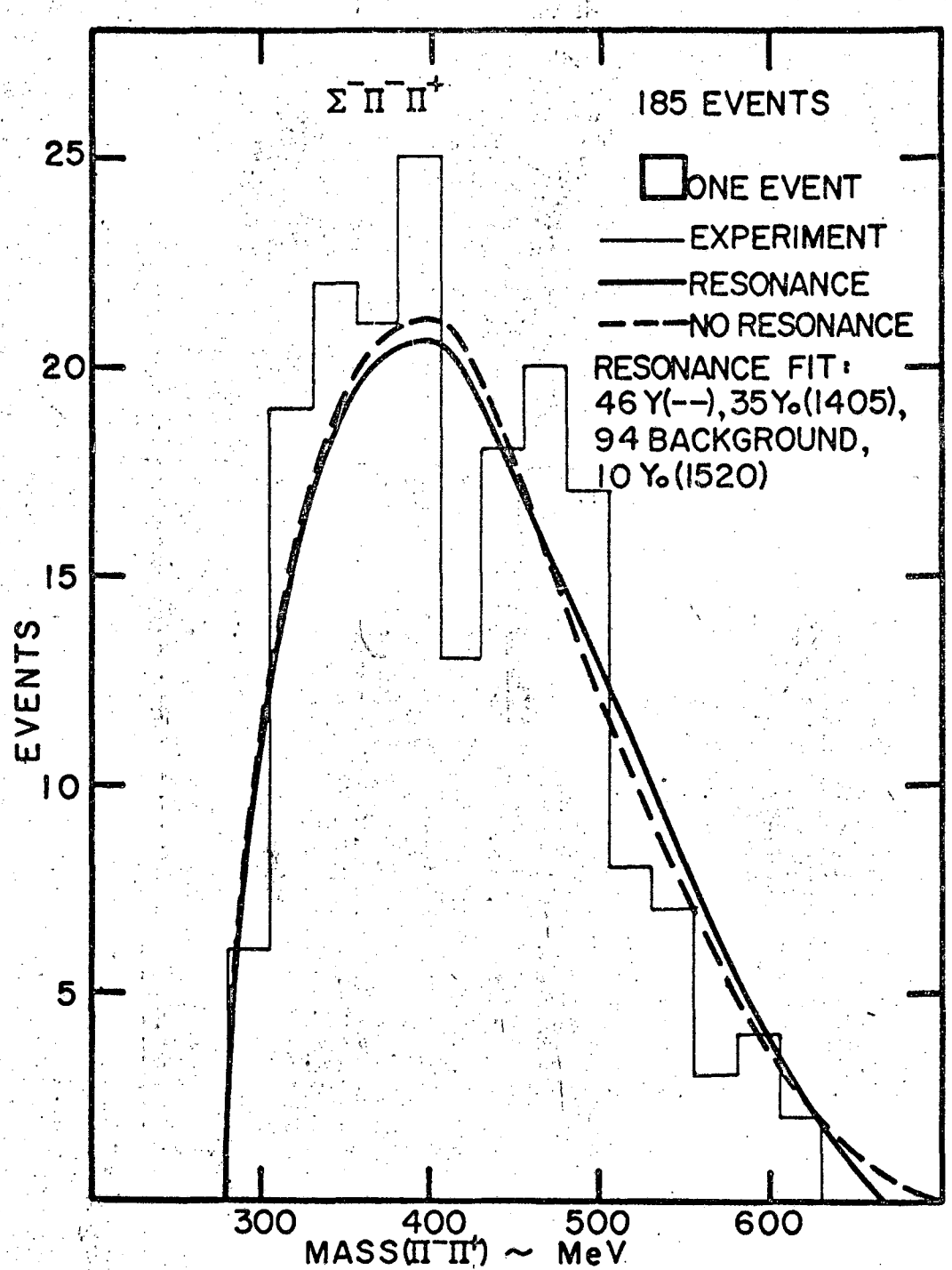

MU-34150

Fig. 22.

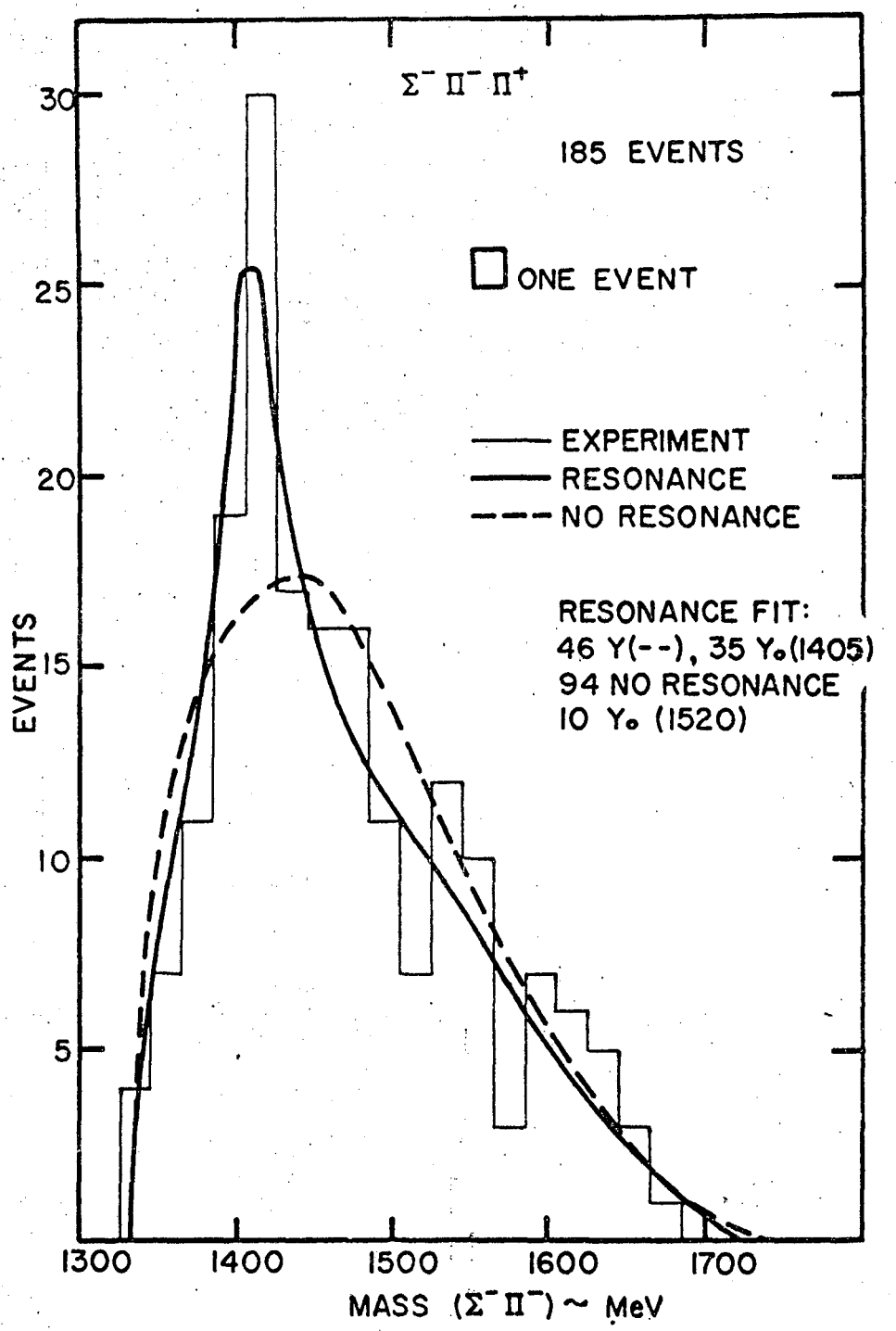

MU-34171

Fig. 23.

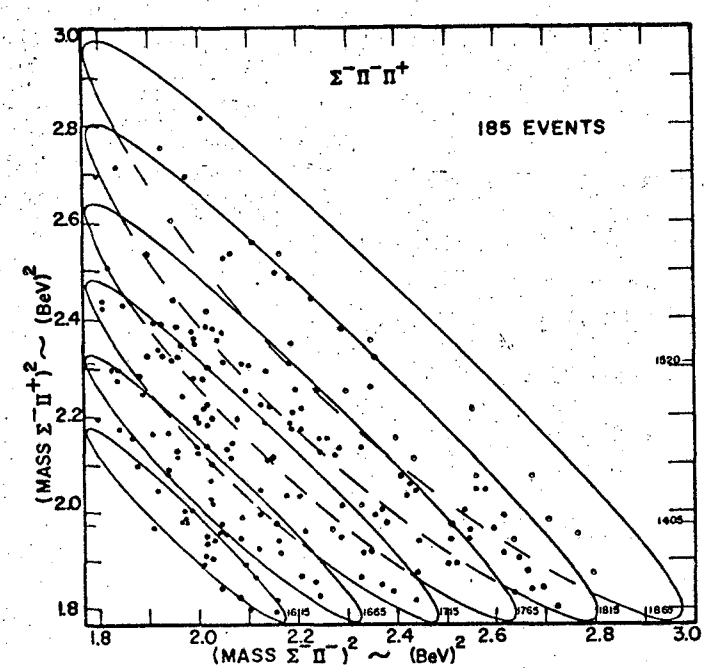

MU-34145

Fig. 24.

invariant mass plot, Figure 17, indicates that this enhancement probably cannot be attributed to carbon production effects.

We will now try to find out what kind of bias, contamination, or other effects in this experiment can give the sharp peak observed.

2) Scanning Bias

We were biased against events where the pion tracks from the sigma decays were steep in the chamber. When we removed this bias by taking only events between 45 and 90 degrees (Figure 6) the peak persisted and, in fact, became more pronounced. These invariant mass distributions with the bias removed are shown in Figure 25.

3) Contamination

In our scanning we found 181 events of the following types:

$$\Sigma^+ \pi^+ \pi^-$$

$$\Sigma^+ \pi^+ \pi^- p$$

$$\Sigma^- \pi^+ \pi^+$$

$$\Sigma^- \pi^+ \pi^+ p$$

These events most likely came from the charge exchange of one pion in carbon in the following reactions:

$$K^- + p \rightarrow \Sigma^\pm + \pi^\mp + \pi^\circ$$

$$K^- + p \rightarrow \Sigma^\pm + \pi^\mp + \pi^+ + \pi^-$$

$$K^- + p \rightarrow \Sigma^\pm + \pi^\mp + \pi^\circ + \pi^\circ$$

The same number of events can charge exchange into the $\Sigma^\pm \pi^\mp \pi^-$ channels.

To see if the peaking could have been due to this contamination, we plotted all the relevant quantities. In the plot of the three-body invariant mass, Figure 26, we found that only about one-third of these events are in the region used in our $\Sigma^\pm \pi^\mp \pi^-$ data (1600 MeV to 1865 MeV).

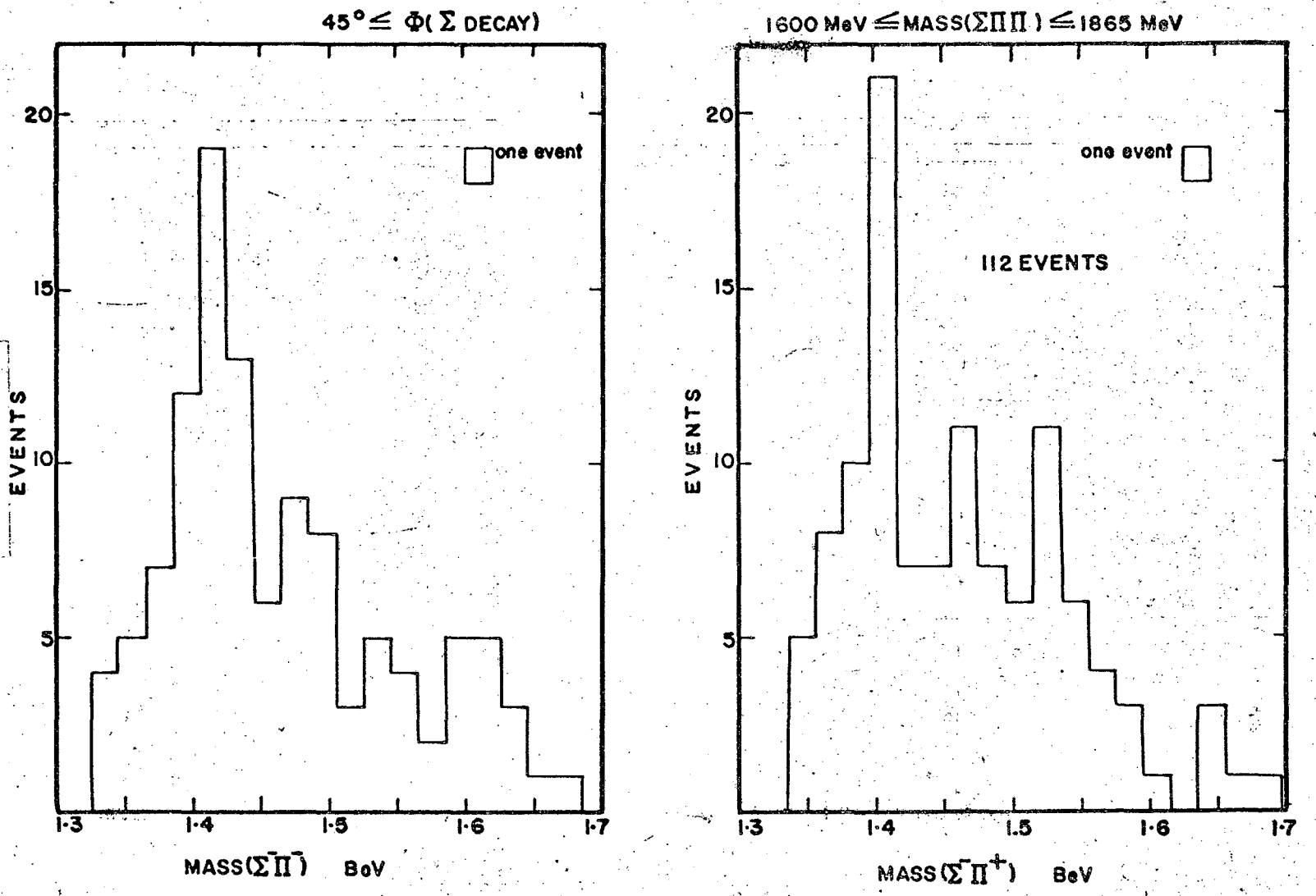

Fig. 25.

MU-34388

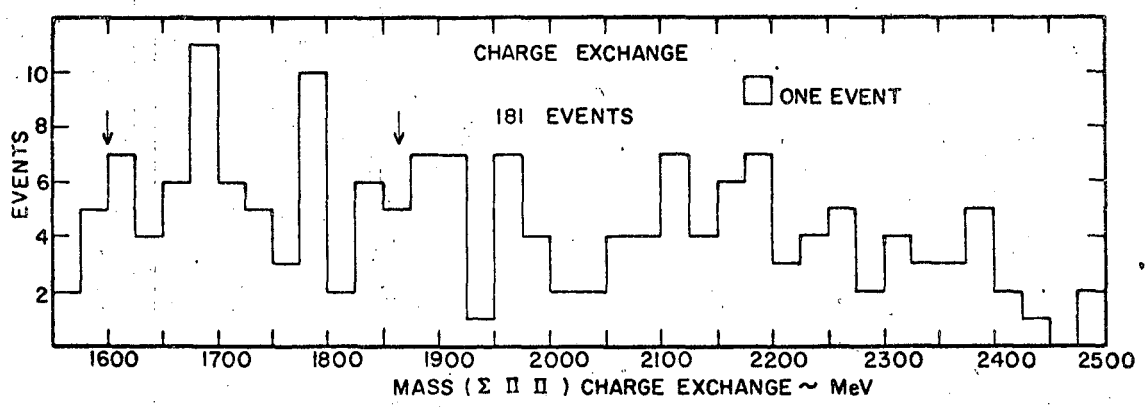

MU-34138

Fig. 26.

This shows that the maximum possible contamination is 64 events.

When we look at the invariant mass plots of the sigma-pion system, Figure 27, we see nothing extraordinary. The small enhancement in the $\Sigma^+ \pi^+$ invariant mass plot at 1405 MeV is probably due to statistics. Of course, this may be a resonance produced in these reactions. But if we assume that this is not due to resonance production, and is not due to statistics, we can subtract this contamination from the $\Sigma^- \pi^-$ invariant mass plot. This would be the maximum amount of contamination. Even after the subtraction, the $\Sigma^- \pi^-$ invariant mass plot is still left with a sharp peak at 1415 MeV. This enhancement cannot be explained away by invoking charge exchange effects.

4) Kinetic Energy Distributions

Some of the Y^*'s which decayed in the carbon nucleus were moving slowly. Evidence of this would be a peak in the laboratory kinetic energy distribution of the pion from the Y^* decay. This peak would exist even if the pion underwent elastic scattering before escaping from the carbon nucleus. For a Y^* with a mass of 1415 MeV, the peak in the laboratory kinetic distribution of the pion from the Y^* decay should appear at approximately 70 MeV.

We calculated the total kinetic energy of the three particle system in the laboratory system for the $\Sigma^- \pi^- \pi^+$ events (Figure 28). We divided the events into two groups to see the possible variations of the pion kinetic energy distribution with the total kinetic energy in the laboratory system. One group's total laboratory kinetic energy fell between 350 and 500 MeV; the other between 500 and 720 MeV. The plots of the pion kinetic energy in the laboratory system are shown in Figures 29 and

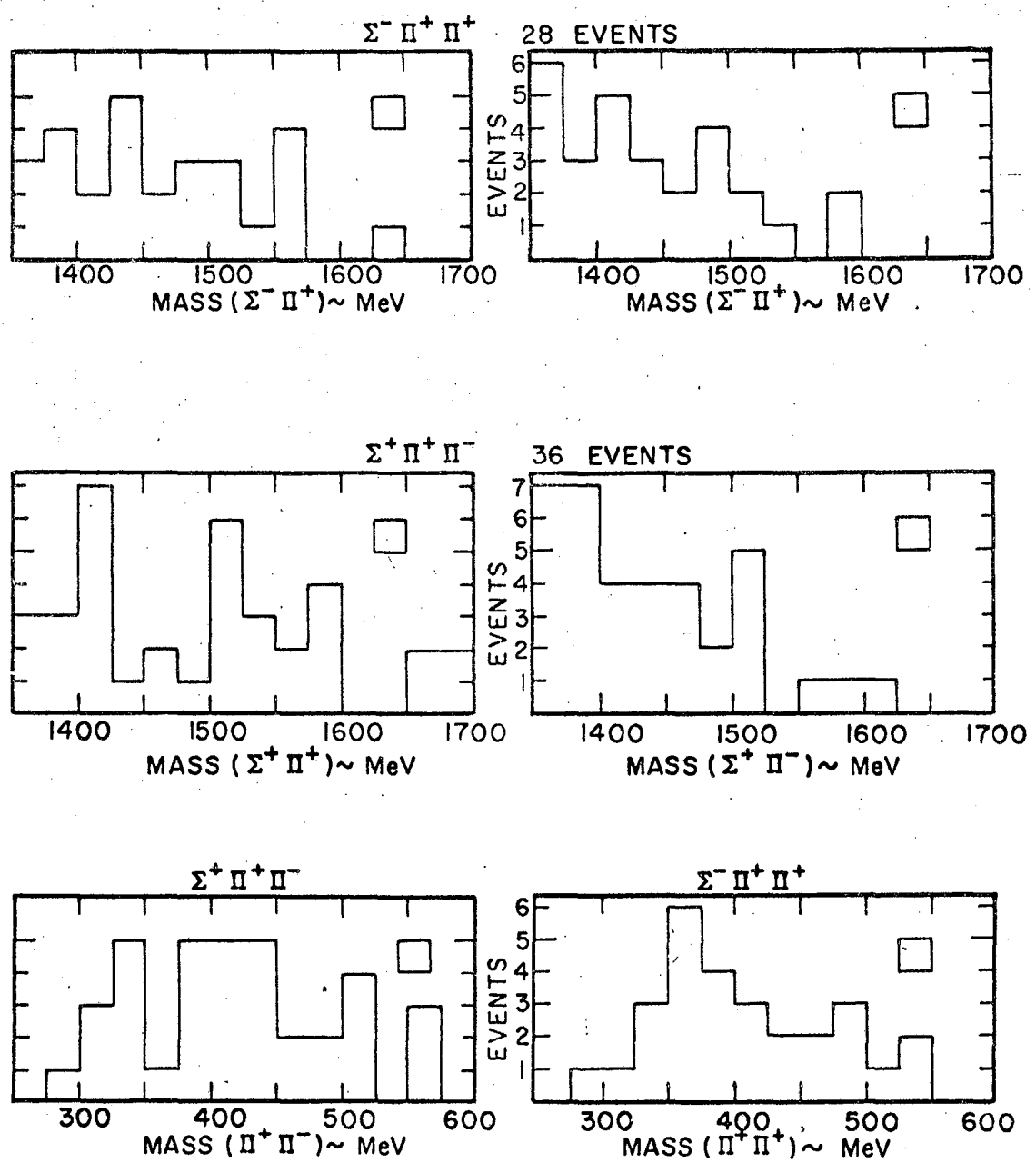

MU-34170

Fig. 27.

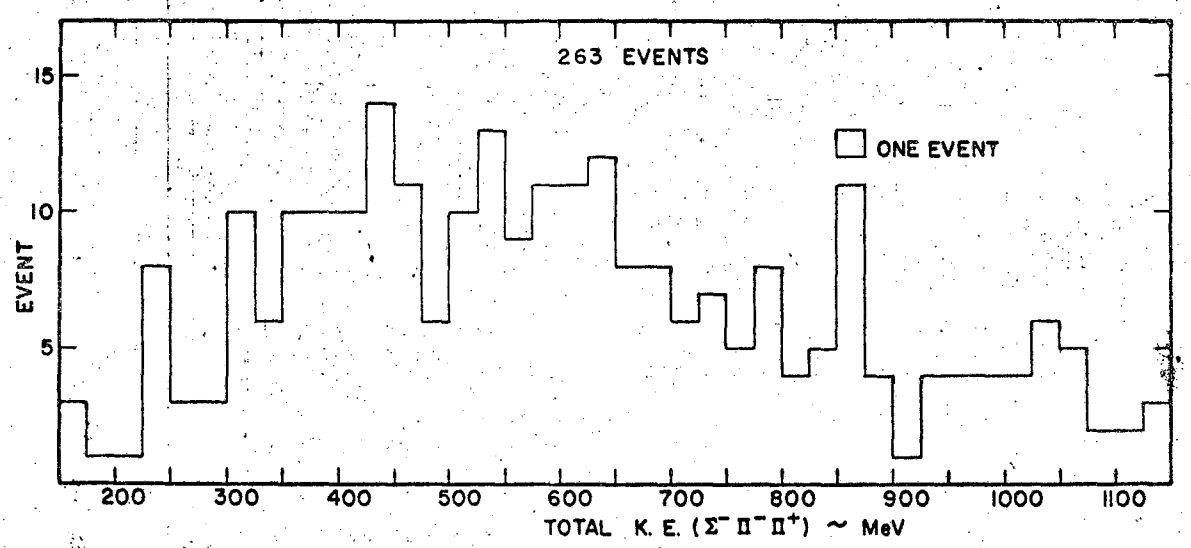

MU-34165

Fig. 28.

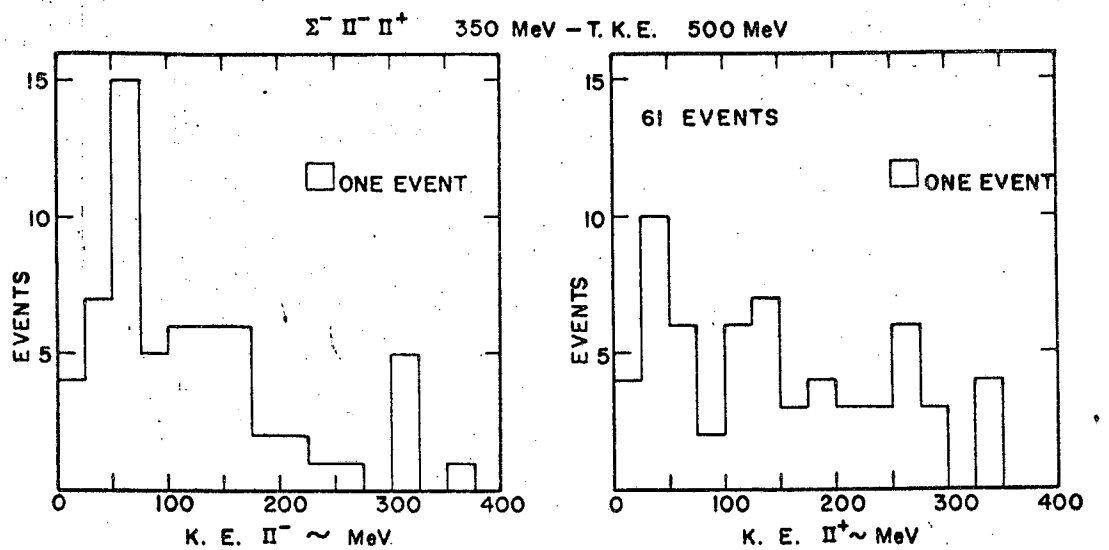
Σ⁻ π⁻ π⁺ 350 MeV – T. K. E. 500 MeV
ONE EVENT
EVENTS
K. E. π⁻ ~ MeV
61 EVENTS
ONE EVENT
EVENTS
K. E. π⁺ ~ MeV
MU-34168

Fig. 29.

30. There appears to be no variation between the two negative pion distributions. The positions of the peaks agree with that of the decay of a 1415 MeV Y^* which is at rest or moving very slowly. When similar procedure was carried out for the $\Sigma^+ \pi^+ \pi^-$ and $\Sigma^+ \pi^+ \pi^- p$ events, we observed no peaking in the positive pion kinetic energy distributions.

A Y^* with a mass of 1415 MeV and a width of 50 MeV would travel about 2 fermis in one mean-life. Using 3 fermis as the radius of the carbon nucleus, we found the average path length to be about 4 fermis. From known K^-N cross sections,[21] we calculated the average path length for K^- before interaction in carbon to be of the order of 2.1 fermis. This left an average path length in carbon of 1.9 fermis for the secondary particles produced. Thus, on the average, one-third of the Y^*'s would get out of the carbon nucleus before decaying. We would see these events in the invariant mass plot. Some of the sigmas and pions from a Y^* which decayed in carbon would escape from the nucleus without interaction. We would see these events in the invariant mass plot also. We estimate that approximately one-half of the Y^*'s produced would be observed in this fashion. Part of the remaining events may be observed by plotting the pion kinetic energy distributions.

When the $\Sigma^- \pi^-$ invariant mass was plotted for the events with the negative pion laboratory kinetic energy between 50 and 75 MeV, the distribution looked like the phase space without resonance. This shows that the events in the pion kinetic energy peak were not the same events observed in the $\Sigma^- \pi^-$ invariant mass peak. We believe these events are those wherein the sigma-pion resonance was produced and then decayed in the carbon nucleus. When these events were subtracted from the invariant mass plot, the peak became more pronounced.

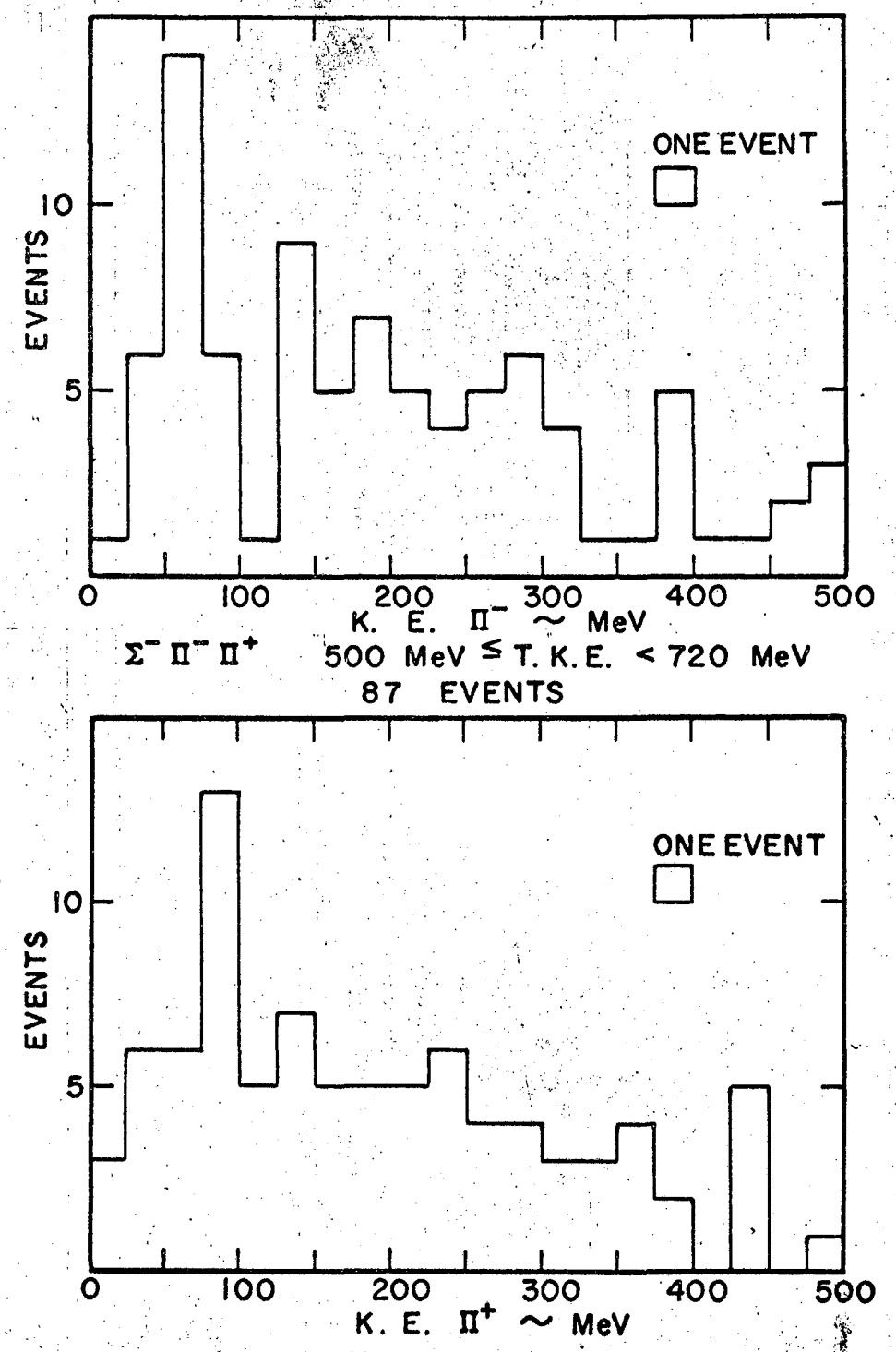

MU-34169

Fig. 30.

Since the invariant mass of the three-particle system does not necessarily have a one-one correspondence with its total laboratory kinetic energy in our experiment, we plotted the sigma-pion invariant mass with the total laboratory kinetic energy cuts stated above (Figures 31 and 32). Although low on statistics, we notice that the peaking is essentially in the 350 MeV to 500 MeV cut. But this should not be suprising, since, as we see from the Dalitz plot (Figure 24), the main contribution to the peak is in the 1700 to 1800 MeV total invariant mass interval. This corresponds approximately to the kinetic energy cut.

5) Reflection

To check the possibility that this peak is due to reflection of resonances not in the sigma-pion or pion-pion systems, we chose the most plausible reaction, that is: $K^- + 2N \rightarrow \Sigma + \pi + N^*_{33}$. Figure 33 shows the phase spaces calculated for this process. It is highly improbable that this will give the sharp peaking observed.

Since no simple interference effects are known to give the sharp enhancement observed and the excess is more than 3 standard deviations from the phase space without resonance, we conclude that the peaking observed is due to a Y^*_2 resonance.

As we pointed out before, there have been enhancements observed in the 1400 MeV region in the $T_3 = |1|$ channel that have been attributed to other effects. In the data at $P_{K^-} = 1.51$ BeV/c,[10] the enhancement at 1415 MeV in the $T_3 = |1|$ system can be explained as the $T_3 = 1$ component of the $T = 2$ resonance.

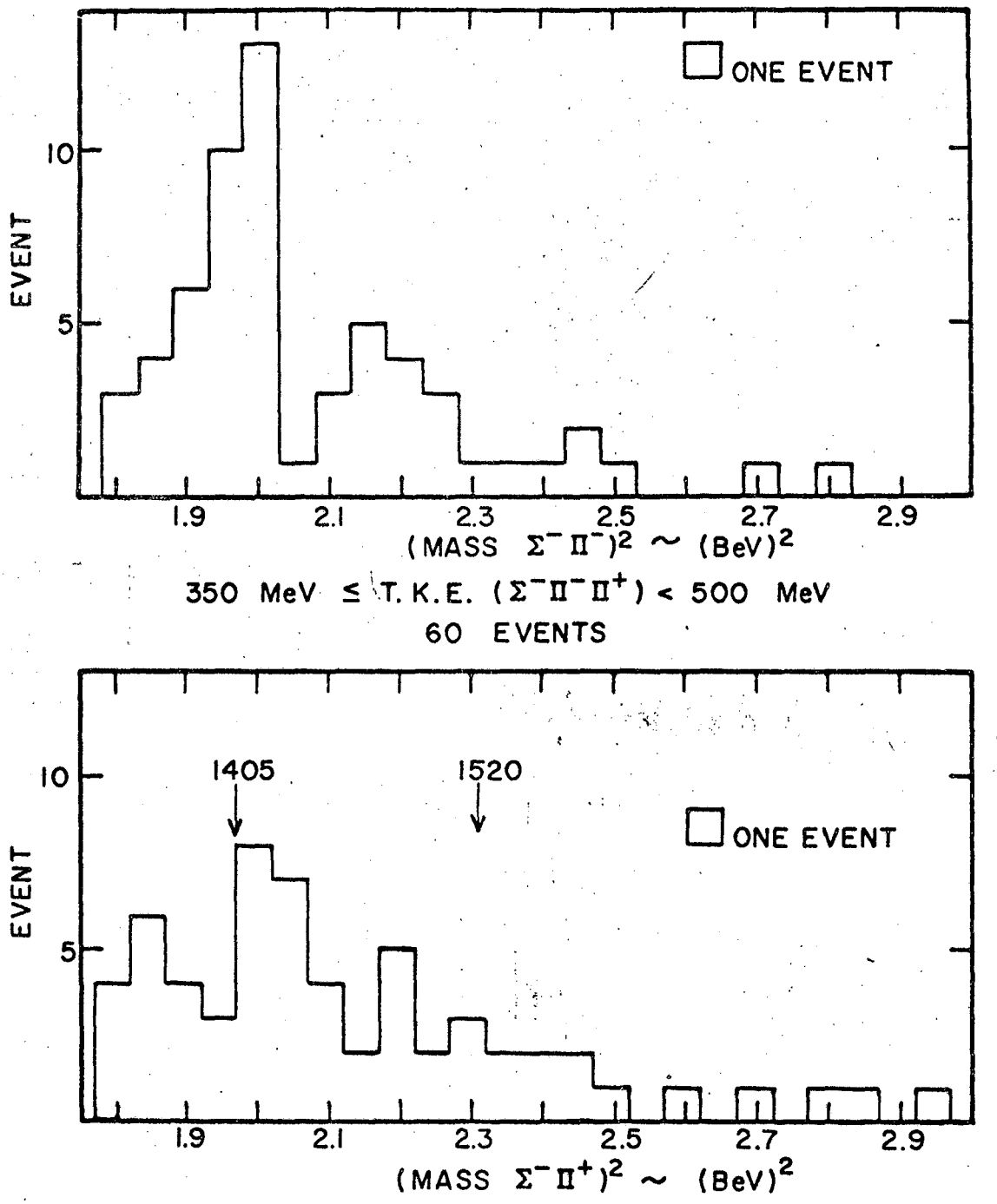

MU-34164

Fig. 31.

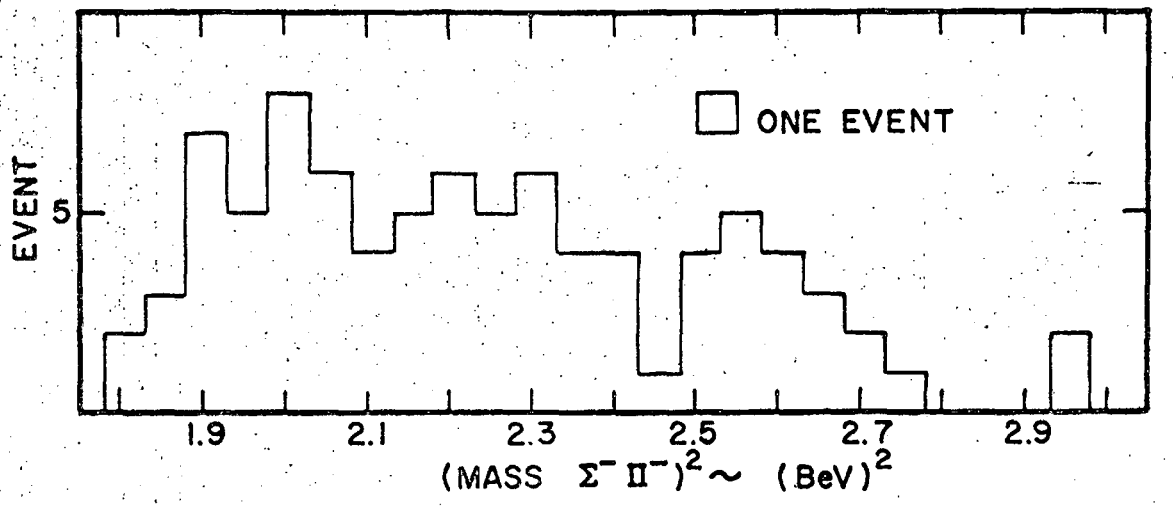

500 MeV $\leq$ T. K. E. $(\Sigma^- \Pi^- \Pi^+) <$ 720 MeV

87 EVENTS

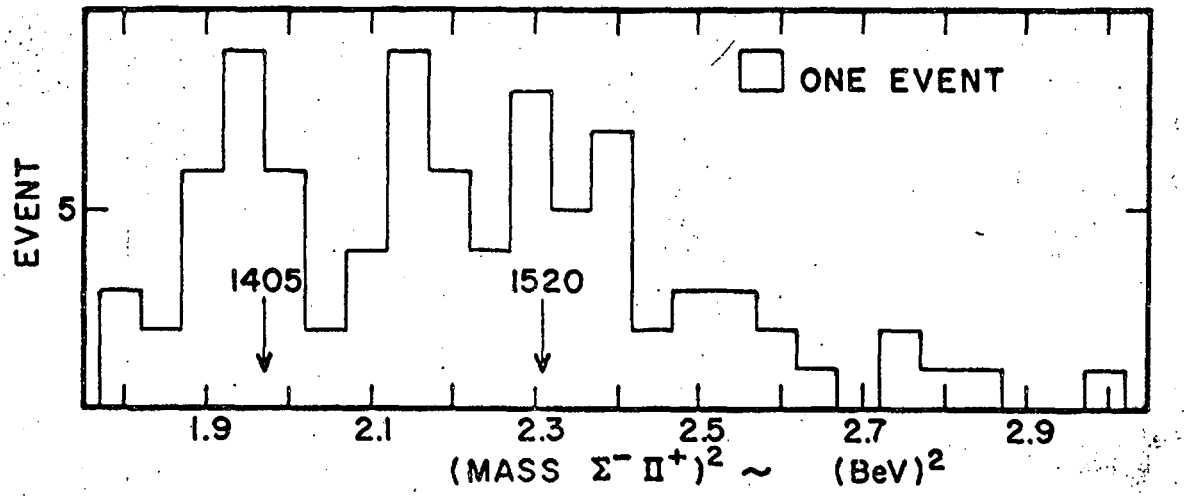

MU-34163

Fig. 32.

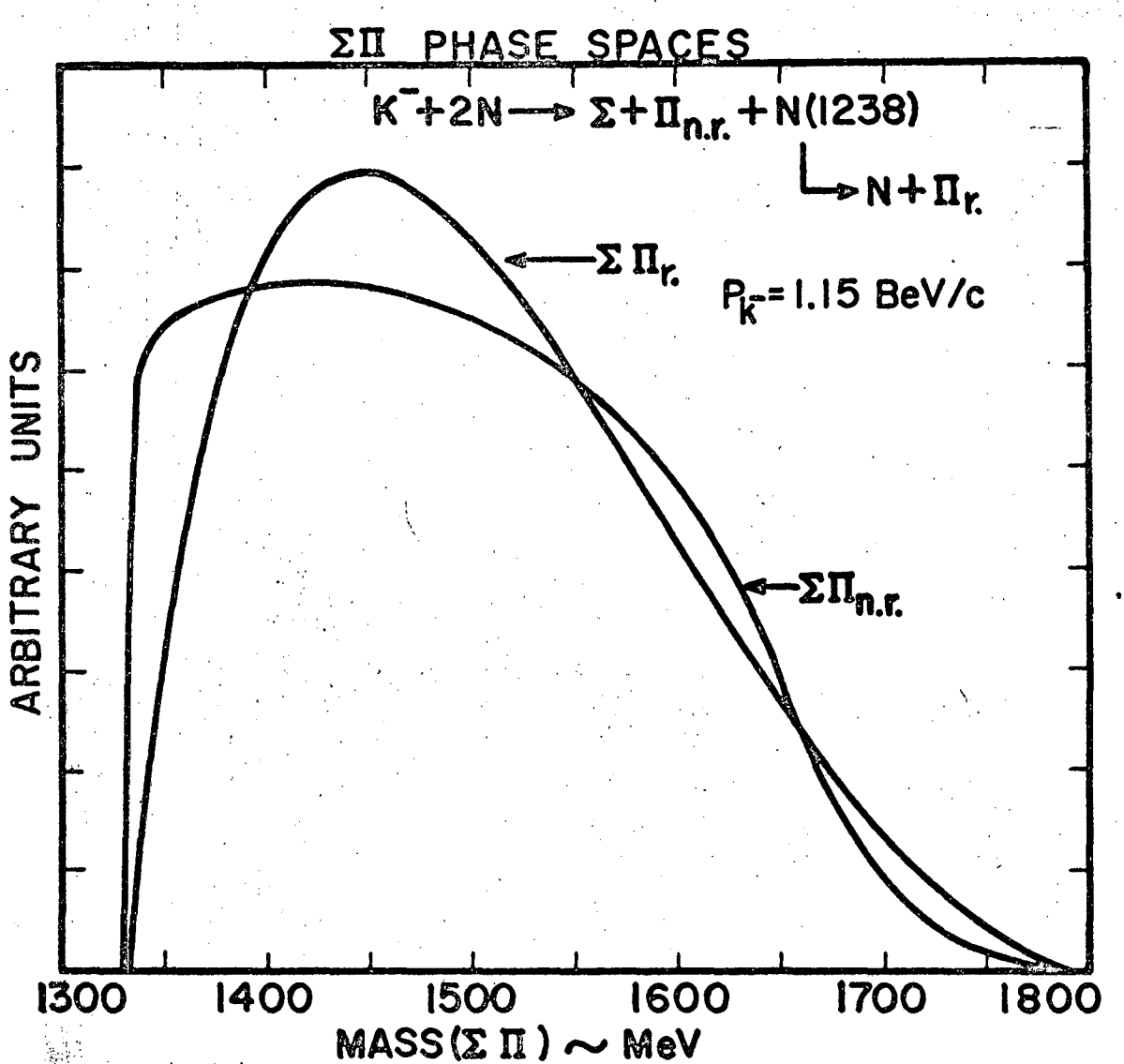

MU-34146

Fig. 33.

X. CONCLUSION

In addition to the well-known Y_0^* (1405), Y_0^* (1520), and Y_1^* (1385), we see an enhancement in the hyperon-two-pion system in the 1750 MeV region. This may be attributed to the Y_1^* (1765).

In particular, we observed a narrow peak in the $\Sigma^- \pi^-$ invariant mass distribution. The Dalitz plot showed that the peak is not due to the reflection of resonances in the $\Sigma^- \pi^+$ or $\pi^- \pi^+$ systems. A comparison with the $\Sigma^+ \pi^-$ invariant mass distribution indicated that this peak probably cannot be attributed to carbon production effects. We found that all the known biases and contaminations of the data did not give this enhancement. No simple interference phenomena are known to give the sharp peaking observed. Further, the departure from the non-resonating phase space is more than 3 standard deviations. In addition, the laboratory kinetic energy distribution of the negative pion indicated the production of a resonance. Therefore, we concluded that the peak in the $\Sigma^- \pi^-$ system is due to the production of a T = 2 resonance. The mass is 1415 ± 16 MeV. The width is not determined because of the large background involved; but from the approximate fit, it should be of the order of 50 MeV or less. The spin and parity of this resonance have not been obtained because of low statistics and because of the impossibility of getting the proper center-of-mass quantities.

The location of this resonance does not agree with the global symmetry or limited symmetry predictions. If the SU_3 theory is correct, then this is the beginning of a 27 multiplet. There should be 22 other members.

It is interesting to note that there appear to be two resonances

in the 1400 MeV region: one with T = 0 and the other with T = 2. The limited symmetry theory predicted that this would be the case as $f^2_{\Sigma\Sigma}$ falls to zero. If this theory is correct, then there should be a Y_1^* below 1385 MeV.

The cross sections for $\Sigma^- \pi^- \pi^+$ and $\Sigma^+ \pi^- \pi^-$ productions from the K^- + n(c) initial state were found to be 0.51 ± 0.07 mb and 0.45 ± 0.07 mb respectively.

An experiment in deuterium is being done to verify these results.

ACKNOWLEDGMENTS

I would like to thank Professor Wilson M. Powell for his interest, advice, and support throughout most of my graduate studies.

I am deeply indebted to Professor Robert P. Ely and Dr. George Gidal for their guidance, suggestions, and counsel.

Enlightening discussions with Dr. Robert W. Birge, Dr. Sun-Yiu Fung, Dr. Robert T. Pu, Mr. Benjamin C. Shen, and Mr. Thomas Schumann were most profitable.

The help of Dr. Sun-Yiu Fung and Dr. William J. Singleton in programing was invaluable.

It is a pleasure to thank Mr. Howard Borer, Mr. Jack Hohenstein, Mrs. Margaret Morley, Miss Charlotte Scales, and Mr. Robert T. Scully for their participation in the scanning of this experiment.

The measurements were done under the direction of Mr. Paul W. Weber. The Data Handling Group under Mr. Howard White did the computer analysis. To the measurers and programmers -- my sincere thanks.

To many past and present members of the Powell-Birge Group goes my utmost gratitude for their help and encouragement.

The special efforts of Mrs. John Pierce, Mrs. Margaret Morley, and Mr. Robert Schlechter in preparing this manuscript are gratefully acknowledged.

This work was done under the auspices of the U. S. Atomic Energy Commission.

FOOTNOTES AND REFERENCES

1. W. M. Powell, W. B. Fowler, and L. O. Oswald, Rev. Sci. Instr. 29, 874 (1958).

2. A. Barbaro-Galtieri, A. Hussein, and R. D. Tripp, Phys. Letters 6, 296 (1963).

3. M. H. Alston, L. W. Alvarez, P. Eberhard, M. L. Good, W. Graziano, H. K. Ticho, and S. G. Wojcicki, Phys. Rev. Letters 5, 520 (1960).

4. R. P. Ely, S. Y. Fung, G. Gidal, Y. L. Pan, W. M. Powell, and H. S. White, Phys. Rev. Letters 7, 461 (1961); J. B. Shafer, J. J. Murray, and D. O. Huwe, Phys. Rev. Letters 10, 176 (1963).

5. J. D. Dowell, W. Koch, B. Leontic, A. Lundby, R. Meunier, J. P. Street, and M. Szeptycka, Phys. Letters 1, 53 (1962).

6. A. N. Diddens, E. W. Jenkins, T. F. Kycia, and K. F. Rieley, Phys. Rev. Letters 10, 262 (1963).

7. G. Alexander, G. R. Kalbfleisch, D. H. Miller, and G. A. Smith, Phys. Rev. Letters 8, 447 (1962); G. Alexander, L. Jacobs, G. R. Kalbfleisch, D. H. Miller, G. A. Smith, and J. Schwartz, in Proceedings of the 1962 International Conference on High-Energy Physics at CERN (CERN, Geneva, 1962), p 320.

8. G. R. Kalbfleisch, G. Alexander, O. I. Dahl, D. H. Miller, A. Rittenberg, and G. A. Smith, Phys. Letters 4, 225 (1963).

9. M. H. Alston, L. W. Alvarez, P. Eberhard, M. L. Good, W. Graziano, H. K. Ticho, and S. G. Wojcicki, Phys. Rev. Letters 6, 698 (1961).

10. M. H. Alston, L. W. Alvarez, M. Ferro-Luzzi, A. H. Rosenfeld, H. K. Ticho, and S. G. Wojcicki, in Proceedings of the 1962 International Conference on High-Energy Physics at CERN (CERN, Geneva, 1962), p 311.

11. M. H. Alston, A. Barbaro-Galtieri, A. H. Rosenfeld, and S. G. Wojcicki, A Search for Y_2^* Resonances, UCRL-11137, Jan., 1964.

12. P. L. Bastien, M. Ferro-Luzzi, and A. H. Rosenfeld, Phys. Rev. Letters 6, 702 (1961).

13. L. T. Kerth and A. Pais, On the Gentle Art of Hunting Bumps, UCRL-9706, May 19, 1961.

14. D. Amati, A. Stanghellini, and B. Vitale, Nuovo Cimento 13, 1143 (1959); Phys. Rev. Letters 5, 524 (1960).

15. The theory also predicts widths and branch ratios into the final state channels, but the dependence on the mass difference, coupling constants, and other parameters like cutoff energy is non-trivial. For details, see Reference 14.

16. S. Okubo, Progr. Theoret. Phys. (Kyoto) 27, 949 (1962); M. Gell-Mann, Cal. Tech. Synchrotron Lab. Report CTSL-20; Phys. Rev. 123, 1067 (1962).

17. P. Eberhard, M. L. Good, and H. K. Ticho, Rev. Sci. Instr. 31, 1054 (1960).

18. P. Newcomb, Experiment No. 16 Beam Momentum (Intergroup report).

19. J. Shonle, Phys. Rev. Letters 5, 156 (1960).

20. Reference Manuals. FOG CLOUDY FAIR Bubble Chamber Data Processing System. Lawrence Radiation Laboratory Document UCID 1340 (unpublished).

21. L. T. Kerth, Rev. Mod. Phys. 33, 389 (1961).

22. S. Y. Fung, An Analysis of Y_1^* Production by 1.15 BeV/c K^- Beam (Ph.D. Thesis), UCRL-11485, Sept. 1963.

23. L. S. Azhgirey, I. K. Vzorov, V. P. Zrelov, M. G. Mescheryakov, B. S. Neganov, R. M. Ryndin, and A. F. Shabudin, Nuclear Phys. 13, 258 (1959).

24. J. P. Berge, P. Bastien, O. Dahl, M. Ferro-Luzzi, J. Kirz, D. H. Miller, J. J. Murray, A. H. Rosenfeld, R. D. Tripp, and M. B. Watson, Phys. Rev. Letters 6, 557 (1961).

25. When the box size was increased to 40 MeV, the probability for a worse fit became approximately 5% for both distributions.

This report was prepared as an account of Government sponsored work. Neither the United States, nor the Commission, nor any person acting on behalf of the Commission:

A. Makes any warranty or representation, expressed or implied, with respect to the accuracy, completeness, or usefulness of the information contained in this report, or that the use of any information, apparatus, method, or process disclosed in this report may not infringe privately owned rights; or

B. Assumes any liabilities with respect to the use of, or for damages resulting from the use of any information, apparatus, method, or process disclosed in this report.

As used in the above, "person acting on behalf of the Commission" includes any employee or contractor of the Commission, or employee of such contractor, to the extent that such employee or contractor of the Commission, or employee of such contractor prepares, disseminates, or provides access to, any information pursuant to his employment or contract with the Commission, or his employment with such contractor.